MASS WASTING IN THE WESTERN GALAPAGOS ISLANDS

A Thesis

by

HILLARY FAWN HALL

Submitted to the Office of Graduate Studies of
Texas A&M University
in partial fulfillment of the requirements for the degree of

MASTER OF SCIENCE

August 2011

Major Subject: Oceanography

Mass Wasting in the Western Galapagos Islands

MASS WASTING IN THE WESTERN GALAPAGOS ISLANDS

A Thesis

by

HILLARY FAWN HALL

Submitted to the Office of Graduate Studies of
Texas A&M University
in partial fulfillment of the requirements for the degree of

MASTER OF SCIENCE

Approved by:

Chair of Committee,	William Sager
Committee Members,	Niall Slowey
	Robert Weiss
Head of Department,	Piers Chapman

August 2011

Major Subject: Oceanography

ABSTRACT

Mass Wasting in the Western Galapagos Islands. (August 2011)

Hillary Fawn Hall, B.S., University of Washington

Chair of Advisory Committee: Dr. William Sager

Oceanic island volcanoes such as those in the Hawaiian, Canary and Galapagos Islands are known to become unstable, causing failures of the subaerial and submarine slopes of the volcanic edifices. These mass wasting events appear to be the primary source of destruction and loss of volume of many oceanic islands, but our knowledge of mass wasting is still rudimentary in many seamount and island chains. To better understand mass wasting in the western Galapagos Islands, multi-beam bathymetry and backscatter sidescan sonar images were used to examine topography and acoustic backscatter signatures that are characteristic of mass wasting. Observations show that mass wasting plays an important role in the development of Galapagos volcanoes. While volcanic activity continues to conceal the submarine terrain, the data show that four forms of mass wasting are identified including debris flows, slumps sheets, chaotic slumps, and detached blocks. A total of 23 mass wasting features were found to exist in the western Galapagos Islands, including fourteen debris flows with one that incorporated a set of detached blocks, seven slump sheets, and one chaotic slump. Some of the indentified features have obvious origination zones while the sources of others are not clearly identifiable. Approximately 73 percent of the surveyed coastlines are

affected by slumping on the steep upper slopes and ~64 percent are affected by debris flows on the lower slopes. Unlike the giant landslides documented by GLORIA imagery around the Hawaiian Islands, the western Galapagos Islands appear to be characterized by small slump sheets existing along the steep shallow submarine flanks of the island and by debris flows that are flanked by rift zones and extend off the platform. This study indicates that submarine mass wasting is widespread in the western Galapagos, suggesting that the production of small-scale downslope movement is part of the erosive nature of these oceanic volcanic islands.

DEDICATION

I dedicate this thesis to my family.

To my parents, Robert and Barbara, and my brother, Jason, for their unconditional love and inspiration. To Theresa and Phillip Milligan for their encouragement and support through all of my schooling. To Manav Vashisth for always being by my side and putting me back on track whenever I started to go astray. I would also like to dedicate this thesis to the memory of my grandmother Irma, who will be always in my heart.

This work is for all of you.

ACKNOWLEDGEMENTS

I would like to thank my committee chair, Dr. Sager, and my committee members, Dr. Slowey, and Dr. Weiss, for their guidance and support throughout the course of this research.

I also want to extend my gratitude to the following organizations and people: The University of Washington Department of Oceanography for the opportunity to participate in research in the Galapagos Islands during the TN189 cruise aboard the *R/V Thomas G Thompson*, Mark Holmes at the University of Washington for going above and beyond to help me obtain and analyze my data, and to Jennifer Glass for answering questions and keeping me in the loop. Thanks also go to my friends and colleagues and the department faculty and staff for making my time at Texas A&M University a great experience.

TABLE OF CONTENTS

Page

LIST OF FIGURES

FIGURE Page

LIST OF TABLES

1. INTRODUCTION

1.1 Background Information

The Galapagos Island Archipelago, a chain of hot-spot produced volcanoes, are located 1000 km off the northwest coast of South America [*Wilson and Hey*, 1995]. Recent radiometric dating studies of Espanola, the oldest and longest dormant island, show that some of the islands have been present for at least the last 3.3 Ma [*Bailey*, 1976]. The oceanic crust that the islands are built on is not older than 10 Ma [*Simkin*, 1984] and therefore the islands must be younger. The spacing and locations of the volcanoes in the western Galapagos Islands can be seen in Figure 1. For the purpose of this investigation the area defined as the western Galapagos Islands is the area of the archipelago that lies to the west of Santa Cruz and Santiago islands. The youngest and most active volcanoes in the archipelago are located on Isabela and Fernandina Islands, which are located at the western edge of the platform due to eastward movement of the Nazca Plate relative to the Galapagos hot-spot [*Gripp & Gordon*, 2002]. While the Galapagos Islands have many active volcanoes, Fernandina Island's Le Cumbre volcano is the most active in the archipelago with greater than 20 witnessed eruptions in the past two centuries [*Simkin and Siebert*, 1994], the most recent in April 2009. Continued volcanism off the west coast of Fernandina and Isabela Island acts to cover the seafloor [*Geist et al*., 2006].

Though these islands are geologically young and continue to erupt and grow larger, the steep cliff faces of the shorelines indicate that the islands have begun to

---

This thesis follows the style of *Geochemistry, Geophysics, Geosystems.*

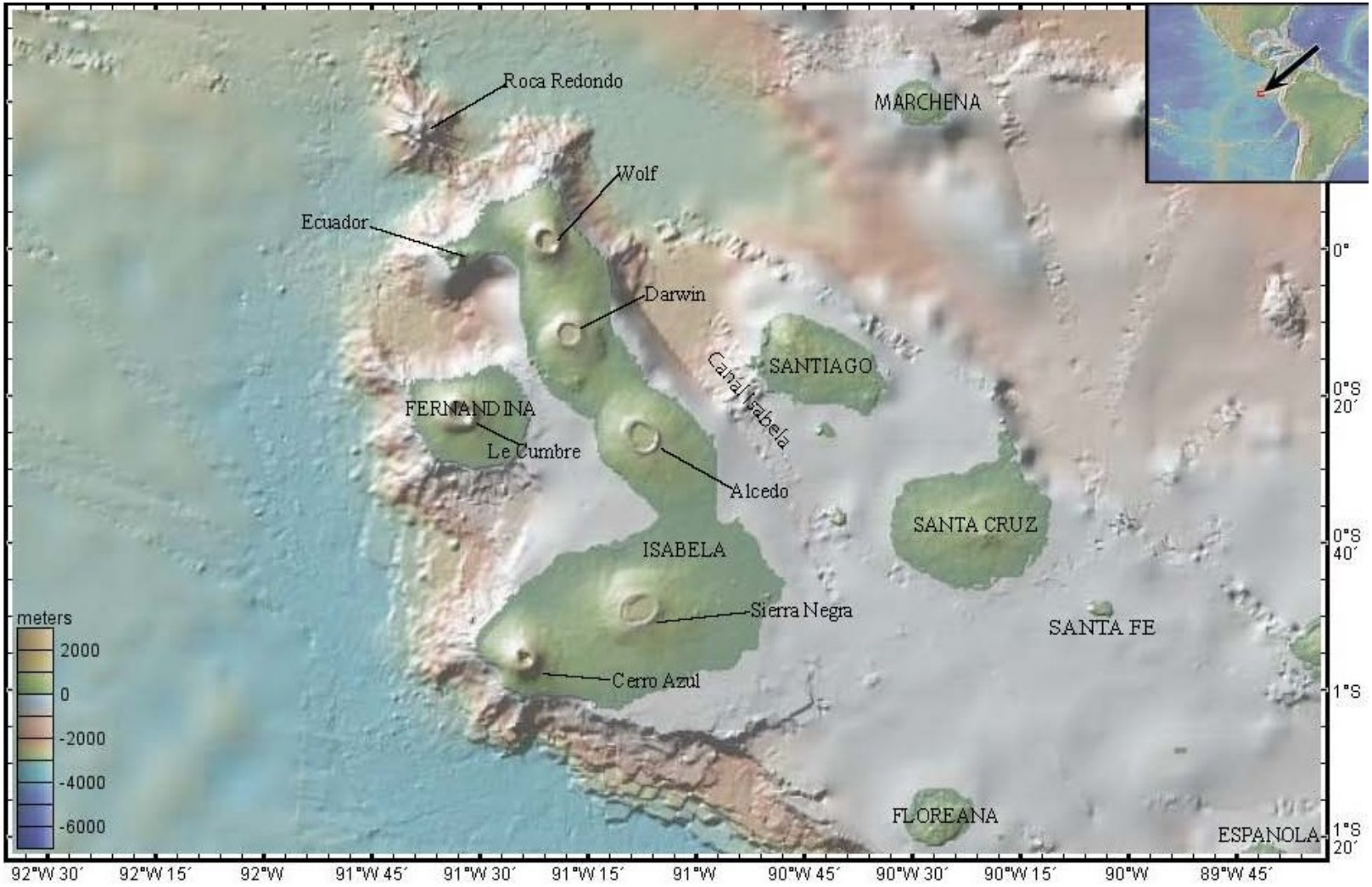

Figure 1. Map of the Galapagos Islands with island and volcano names and identifying Canal Isabela. Inset shows location with respect to North and South America. Data obtained from MGDS GeoMap App.

experience mass wasting. Mass wasting is defined as the downhill movement of soil and rock under the influence of gravity. *Coleman and Prior* [1988] state that the following types of mass wasting are common to the subaqueous environment: 1) falls which are defined as the free-fall of rock, mud or sand sized particles which are restricted to very steep, near-vertical underwater slopes, 2) slides which are defined as the movement of a sediment mass along discrete basal shear planes, 3) debris flows which consist of sediment containing larger clasts that are supported in a matrix, 4) liquefaction flows which occur when loosely packed, coarse grained sediment collapses, and 5) turbidity flows which occur due to a downslope transport of sediment that is supported by an upward component of fluid turbulence. *Moore et al.* [1989] described debris avalanches as material generated by collapse along listric faults and they noted that a slump is generated by the slow ocean-ward movement of a portion of the volcanic flank. *Keating et al*. [2000] described chaotic slumping as downslope movement with a highly disorganized morphology and often contain detached blocks composed of massive slide blocks that remain intact during downslope movement. The debris avalanches and slumps described by *Moore et al*.[1989] and the chaotic slumping and detached blocks described by *Keating et al*. [2000] are all considered specific examples of slide types within the spectrum defined by *Coleman and Prior* [1988].

The most commonly identified form of mass wasting on oceanic islands is slides and a variable range of sizes have been found in seafloor images obtained by surveying the submerged flanks of volcanic islands [*Holcomb and Searle*, 1991; *Lenat et al*.,1989; *Moore et al.,* 1989]. In oceanic island volcanoes, these slides can be characterized by a

headwall scar and a displaced mass [*Hampton et al*., 1996]. Giant slides are well documented on the Hawaiian Ridge [*Moore*, 1964; *Fornari et al.*, 1979; *Moore et al.*, 1989], in the Canary Islands [*Holcomb and Searle*, 1991; *Watts and Masson*, 1995; *Stillman*, 1999] and at Reunion Island [*Lenat et al*., 1989; *Gillot et al*., 1994]. A number of factors are thought to cause the stresses that lead to these collapses: volcanic spreading [*Borgia*, 1994], dike intrusions [*McGuire et al*., 1990; *Elsworth & Voight*, 1995], accumulation of eruptive products on steep slopes [*Murray and Voight*, 1996], earthquakes [*Montalto et al*., 1996; *McGuire*, 1996], magma chamber inflation and deflation [*Lo Giudice & Rasa*, 1992], and changing sea levels [*Firth et al*., 1996].

Giant slides in the western Galapagos are not as common as in the Hawaiian Islands; however, they are known to occur. Furthermore, steep cliff faces observed at the southwest flank of Cerro Azul [*Naumann and Geist*, 2000], the west face of Pinta [*Cullen and McBirney*, 1987] and the west face of Santa Fe [*Geist et al*., 1985] can be interpreted as subaerial headwall scars. The halving of Volcan Ecuador, located at the northwestern most tip of Isabela Island, is a particularly dramatic example. *Geist et al*. [2002] state that the entire west half of the volcano slid along a listric fault into the abyssal depths of the platform. This slide generated two distinct slide features, a headwall scar identified in the topography and a debris toe at the base of the slide identified in the bathymetry.

1.2. Previous Work

Using MR-1 sidescan sonar data, *Geist et al.* [2006] and *Geist et al*. [2008] identified five submarine geomorphic provinces in the western Galapagos including

large deep-water lava fields, submarine rift zones, terraces, shallow submarine flanks, and mass wasting and erosional deposits. These articles include detailed figures of the geological interpretations of the sidescan sonar data, indicating all of these five provinces. *Geist et al*. [2006] also indicated that subaerial lava flows have been truncated by wave erosion, producing unstable clastic deposits on over-steepened upper slopes.

Using EM300 bathymetry and MR1 sidescan sonar data, *Glass et al*. [2007] identified volcanic cones of varying morphologies (e.g. pointed, cratered, flat topped and breached), vents, large deep-water lava flows and additional submarine rift zones on Isabela and Roca Redonda islands.

Though *Geist et al.*[2006] and *Glass et al*. [2007] identify mass wasting in the western Galapagos using sidescan sonar data, neither has detailed the types of mass wasting that have occurred. The purpose of this project is to use multibeam bathymetry and backscatter along with sidescan sonar data collected in the western Galapagos Islands to determine the location, size and morphology of mass wasting to better understand its role and to help further the understanding of the geomorphology of the Galapagos Islands. This knowledge will help to understand the way that oceanic island volcanoes erode during their continued growth and evolution as well as determining the size of mass wasting deposits.

2. METHODS

2.1 Data Acquisition

This study is based on sonar-derived bathymetry and backscatter data. These data, which cover the areas shown in Figure 2, were acquired during several research cruises around the islands, including the TN188, TN189 and DRFT04RR cruises. Multibeam bathymetry and backscatter data (Figure 2a and 2c, respectively) were collected during the TN188 and TN189 research cruises onboard the *R/V Thomas G. Thompson* in January 2006 using a Kongsberg Simrad 30 kHz EM300 sonar system. The hull-mounted EM300 transducer array transmits 135 beams per ping with vertical and horizontal resolution approximately 0.2 and 2% of water depth, respectively. Ship navigation was by P-Code GPS and motion sensing/attitude corrections were made with a POS/MV Model 320 vertical reference unit. Additional bathymetry data and sidescan sonar data were obtained from the National Geophysical Data Center (NGDC) and the Marine Geosciences Data System (MGDS) for the 2001 DRFT04RR cruise. This cruise focused on the western edge of the Galapagos platform and collected EM120 multibeam bathymetry and MR1 sidescan sonar backscatter data [*Fornari et al*., 2001; *Kurz et al*., 2001; *Harpp et al*., 2003; *Geist et al*., 2005, 2006] (Figures 2b and 2d, respectively). Methods of data collection are described by *Geist et al.* [2006]. Individual cruise information can be found in Table 1.

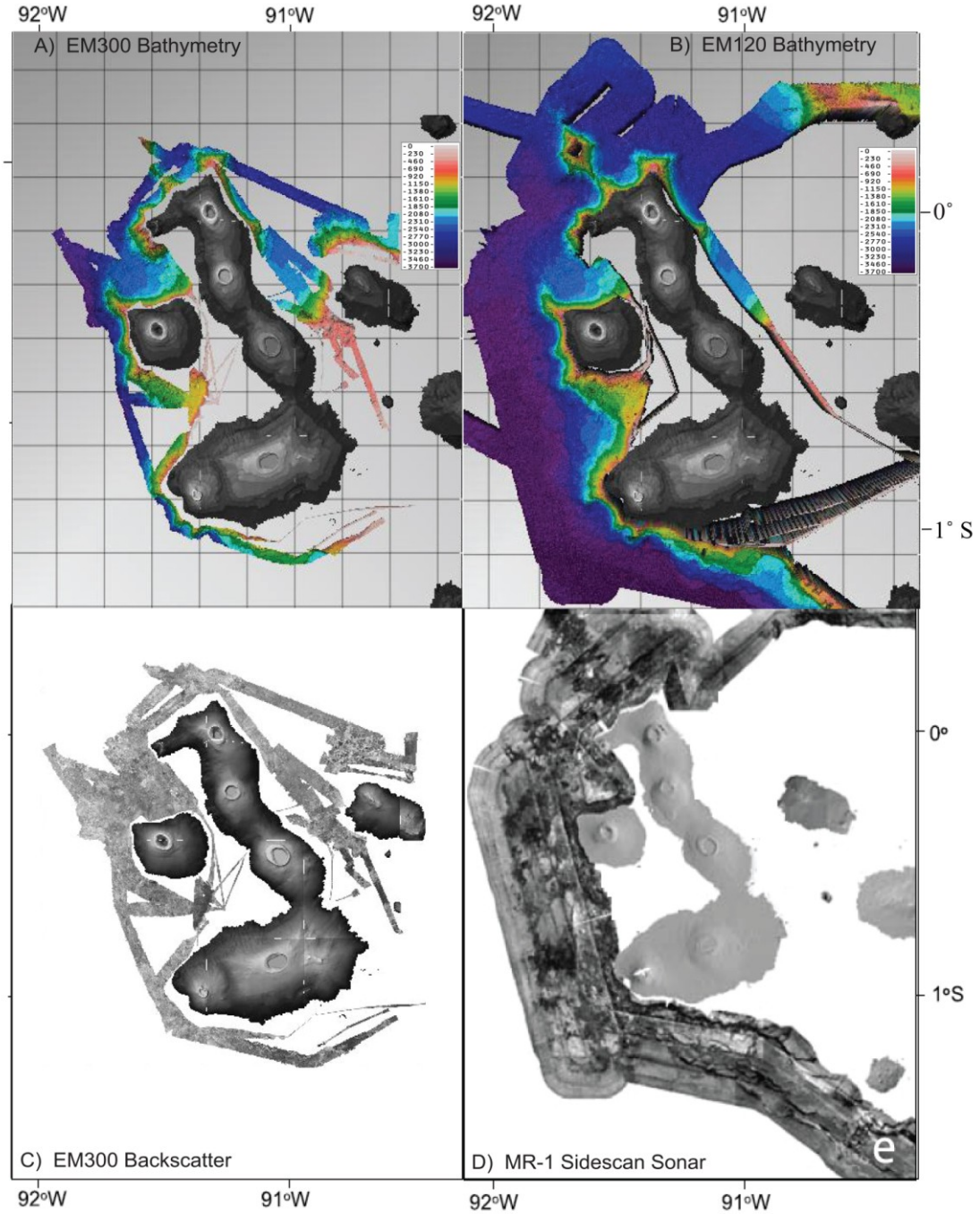

Figure 2. Multibeam bathymetry, backscatter and sidescan sonar data of the western Galapagos. (A) EM300 (25 m resolution) multibeam bathymetry from TN188 and TN189 cruises. (B) EM120 multibeam bathymetry (100 m resolution) from DRFT04RR cruise. (C) EM300 backscatter from TN188 and TN189 (gridded at 25 m resolution) (D) MR1 sidescan sonar data from DRFT04RR cruise (gridded at 8 m resolution). Sidescan images are plotted with dark representing high backscatter and light, low backscatter or acoustic shadow.

Table 1. Cruise Data.

Cruise ID	Ship	Institution	Cruise Dates	Navigation Types	Instrument (primary)
DRFT04RR	Roger Revelle	University of California, Scripps Institution of Oceanography (UC/SIO)	2001-08-23 to 2001-09-25	GPS	Simrad EM120
TN188	Thomas G Thompson	University of California, Santa Barbara	2005-12-03 to 2006-01-10	GPS	Simrad EM300
TN189	Thomas G Thompson	University of Washington, Department of Oceanography	2006-01-12 to 2006-01-26	GPS	Simrad EM300

2.2 Data Processing

EM300 bathymetry data collected during the TN188 and TN189 cruises were cleaned using *Caris* software. This software was used to open and view the soundings received by the Simrad EM300 and to remove soundings that seems to be outliers, i.e., out of place and artificial. The recognition of outlier data was based on knowing roughly the bathymetry of the study area and being able to recognize when soundings do not fit a smooth curve or appear out of place. After the data were cleaned, a grid of some resolution was created that was exported out of *Caris* as a .xyz file. A low resolution grid, 100 m in this case, was chosen to begin with to ensure that all data are included into the grid and no interpolation was necessary. A gridded digital bathymetry model (DBM) was generated from the .xyz files using *Fledermaus*. Using the

Fledermaus software package, an analysis was run on the gridding to determine if a higher resolution could be obtained. In this study, after analysis of the gridding, a final resolution of 25 meters was chosen for the EM300 bathymetry data.

The backscatter data were loaded into *GeoCoder* where they were gridded and a mosaic was created which was exported as a .tiff file. MR1 sidescan sonar data collected during the DRFT04RR cruise have been plotted with the convention that dark represents high backscatter and light is low backscatter or acoustic shadow.

2.3 Data Interpretation

Geist et al.[2006] indicated that areas of mass wasting in the western Galapagos Island can be identified in the bathymetry record as areas of smooth, steep slopes with moderate to low backscatter amplitude and downslope lineations in the sidescan data. In GLORIA sonograph imagery taken in the Canary Islands, *Holcomb and Searle* [1991] described a speckled or mottled backscatter pattern that is indicative of large slide deposits where each speckle represents a blocky hillock.

The DBM and mosaics were examined in *Fledermaus* to co-register the EM300 bathymetry with the MR1 sidescan sonar data. The co-registration was completed by identifying features, such as distinctive volcanic cones in both the bathymetry and the sidescan sonar data. The co-registered images were used to identify mass wasting characteristics described by *Geist et al*. [2006] and *Holcomb and Searle* [1991]. The *Fledermaus* images were then exported as ASCII files and opened in *ArcMAP* for determination of lengths, widths and areas of the identified slides. The length, width and areas of the identified slides were determined using the spatial statistics tool in *ArcMap*.

A new polygon, called a "feature" in *ArcMAP*, was created to outline the co-registered slide locations identified in *Fledermaus*. The spatial statistics tool was then used to determine the areas of the new feature while the measure tool was used to determine their lengths and widths at the largest point in the slide. This procedure was completed three times to verify accuracy and as long as the bounds of the feature are clearly defined and remain the same each time, this method can be reproduced and was used to determine the areas of all slides identified in this study. The percent of coastline affected by mass wasting was determined by using the measure tool in *ArcMAP* to determine the total amount of coastline that was surveyed and then to divide the amount of coastline that has mass wasting features by the total amount surveyed. The mass wasting features were measured at their widest point.

For this study, the western Galapagos was divided into five regions based on the presence of mass wasting in the data and these regions were named after the volcanoes located nearest to the region. These regions are identified in Figure 3 and their sizes are based on the division of the bathymetry and sidescan data into a 1:50,000 scale in the 2001 DRFT04RR cruise report [*Kurz et al*., 2001].

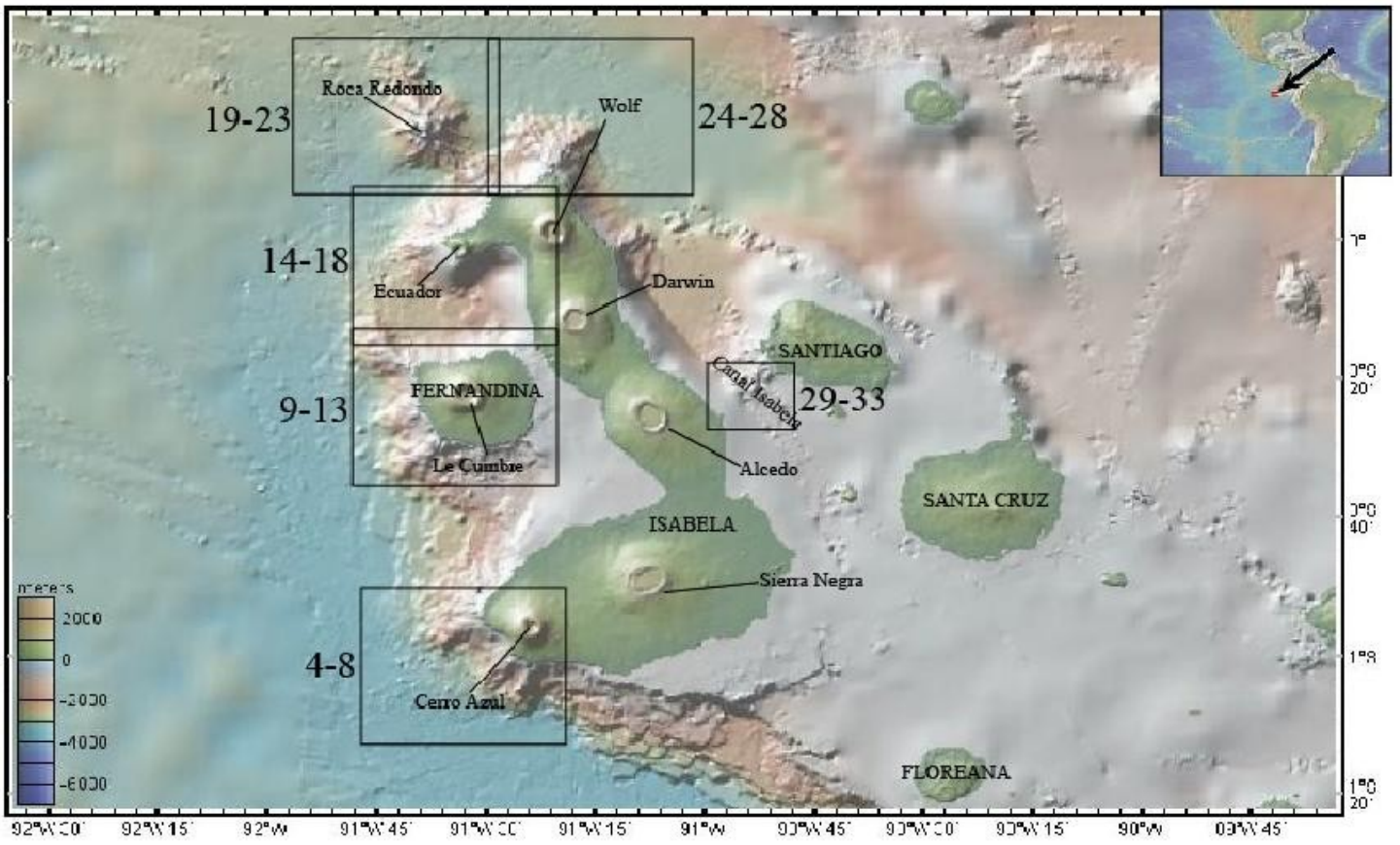

Figure 3. Map of the Galapagos Islands with locations of Figures 4-33. Numbers correspond to subsequent figures.

3. RESULTS

Bathymetry and sidescan data indicate that most volcanic slopes show evidence of mass wasting in the western Galapagos. The data show that four forms of mass wasting are identified including debris flows, slump sheets, chaotic slumps, and detached blocks. Debris flows are identified in the sidescan sonar data as having moderate to low backscatter amplitude and downslope lineations in the sonar images, giving the effect of a streaky appearance. Slump sheets are identified as having moderate backscatter amplitude with folds that give the impression of a rippled appearance in sidescan sonar images. Chaotic slumps are identified as having moderate to low backscatter amplitude with a mottled or speckled appearance in sidescan sonar images. Detached blocks are identified in sidescan sonar images by a margin of high backscatter amplitude, appearing dark in the images, with upper surfaces characterized by low backscatter amplitude, which appear white, indicating acoustic shadow. Submarine rift zones are characterized by highly reflective mottled backscatter in the sidescan sonar data and as linear or gently curving ridges in the bathymetry. Large deep-water lava fields are characterized as irregularly shaped areas of higher reflectivity. The areas of the bathymetric expression of the slides were defined by the existence of horseshoe shaped embayments (concave contours) on the upper slopes and bulges (convex contours) on the lower slopes. Table 2 lists the slide and slump features by both name and acronym and sidescan sonar and bathymetry interpretations of length and width at the widest point as well as the calculated areas.

Table 2. A Listing of Slide and Slump Feature Characteristics.

		Sidescan Sonar			Bathymetry					
	Acronym	Area (km^2)	Length (km)	Width (km)	Area (km^2)	Length (km)	Width (km)	Type	Total Length of Surveyed Coastline (km)	% of Total Area affected
Cerro Azul Region									35.97	
Cerro Azul South Slide	CAS	17.51	7.23	4.60	44.86	10.63	5.11	DF		
Cerro Azul Southwest Slide	CASW	21.32	6.42	4.69	208.31	19.81	15.39	DF		56.99
Slump Cerro Azul	SCA	55.38	33.07	1.83	N/A	N/A	N/A	SS		91.92
Le Cumbre Region									48.92	
Le Cumbre Southwest Slide	LCSW	27.62	10.54	4.03	66.96	12.45	5.02	DF		
Le Cumbre Northwest Slide	LCNW	46.59	10.88	5.02	166.19	12.43	11.37	DF		
Le Cumbre North Slide	LCN	111.98	6.76	14.96	101.29	5.66	16.33	DF		66.91
Slump Le Cumbre West	SLCW	26.89	17.65	1.61	N/A	N/A	N/A	SS		
Slump Le Cumbre North	SLCN	93.72	19.54	1.16	N/A	N/A	N/A	SS		76.03
Volcan Ecuador Region									32.50	
Volcan Ecuador West Slide	VEW	36.30	9.27	5.51	68.22	10.96	7.29	DF w/ DB		
Volcan Ecuador Northwest Slide	VENW	28.36	12.28	4.22	57.44	12.71	5.77	DF		
Volcan Ecuador North Slide	VEN	43.05	7.78	5.71	64.95	10.09	9.03	DF		67.99
Slump Volcan Ecuador West	SVEW	13.57	4.35	2.13	N/A	N/A	N/A	SS		
Slump Volcan Ecuador North	SVEN	56.39	28.14	1.62	N/A	N/A	N/A	SS		100.00

Table 2. Continued

	Acronym	Sidescan Sonar Area (km^2)	Sidescan Sonar Length (km)	Sidescan Sonar Width (km)	Bathymetry Area (km^2)	Bathymetry Length (km)	Bathymetry Width (km)	Type	Total Length of Surveyed Coastline (km)	% of Total Area affected
Roca Redondo Region									34.51	
Roca Redondo Southwest Slide	RRSW	68.40	14.28	6.82	120.82	16.41	10.01	DF		
Roca Redondo Northwest Slide	RRNW	60.96	12.97	6.90	55.81	11.27	6.22	DF		
Roca Redondo Northeast Slide	RRNE	32.72	10.97	6.23	77.05	12.66	10.35	DF		
Roca Redondo Southeast Slide	RRSE	N/A	N/A	N/A	81.04	13.92	7.93	N/A		100.00
Volcan Wolf Region									48.81	
Volcan Wolf North Slide	VWN	91.56	13.23	10.21	88.43	10.36	9.23	DF		
Volcan Wolf East Slide	VWE	57.15	5.71	9.72	162.90	16.34	10.34	DF		40.08
Slump Volcan Wolf North	SVWN	86.26	36.27	2.26	N/A	N/A	N/A	SS		
Slump Volcano Wolf East	SVWE	33.86	7.06	2.53	N/A	N/A	N/A	SS		88.77
Canal Isabela Region									15.70	
Slump Canal Isabela	SCI	70.12	11.37	13.57	93.57	15.23	13.81	CS		
					Total % Area Covered in Slides					**64.47**
					Total % Area Covered in Slumps					**72.76**

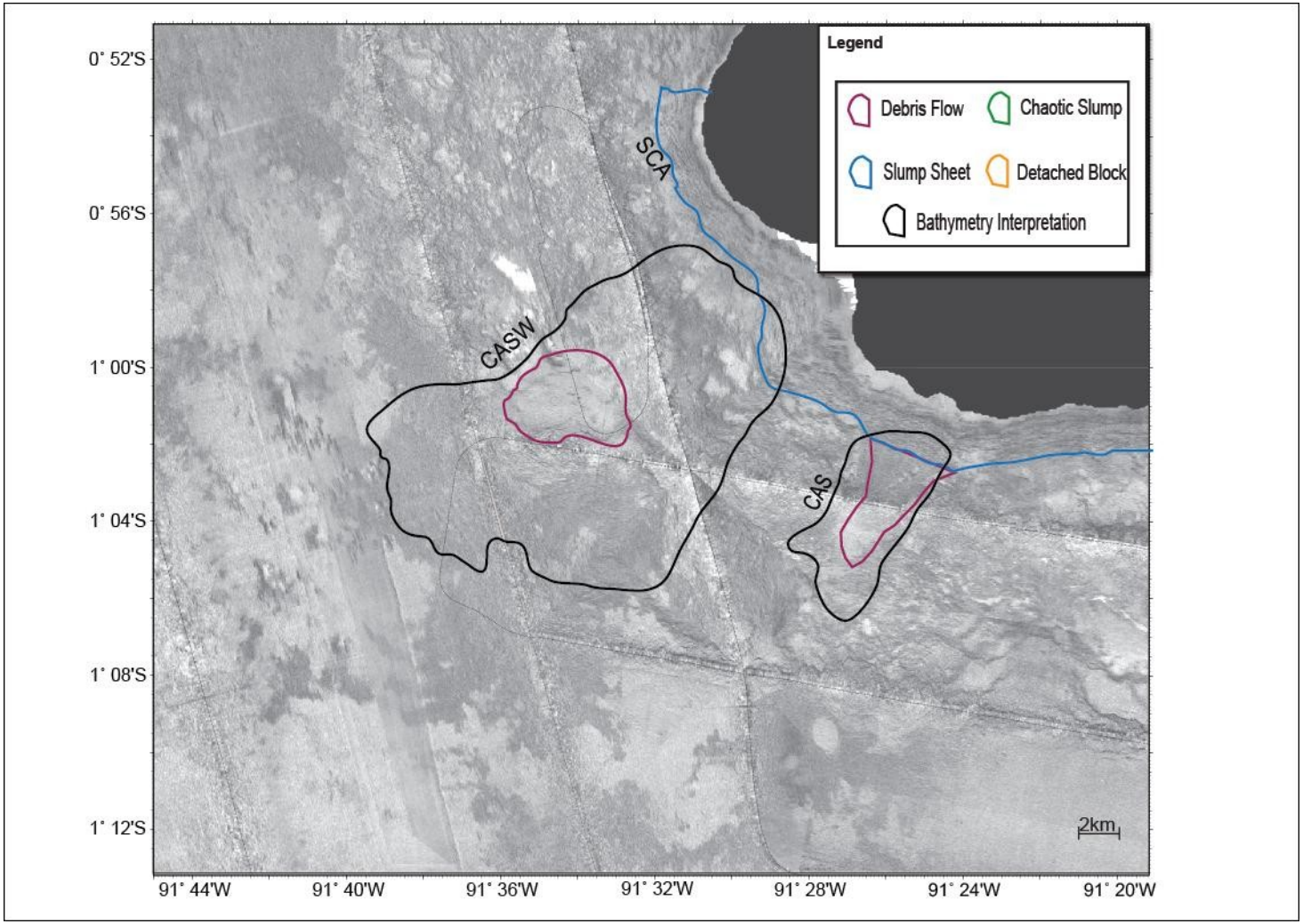

Figure 4. Cerro Azul sidescan sonar data interpreted. Interpretations include slump sheets outlined in blue and debris flows outlined in red, with bathymetry interpretations outlined in black. High backscatter plotted in dark tone and low backscatter or acoustic shadow as light tone. Islands shown in grey. Location shown in Figure 3.

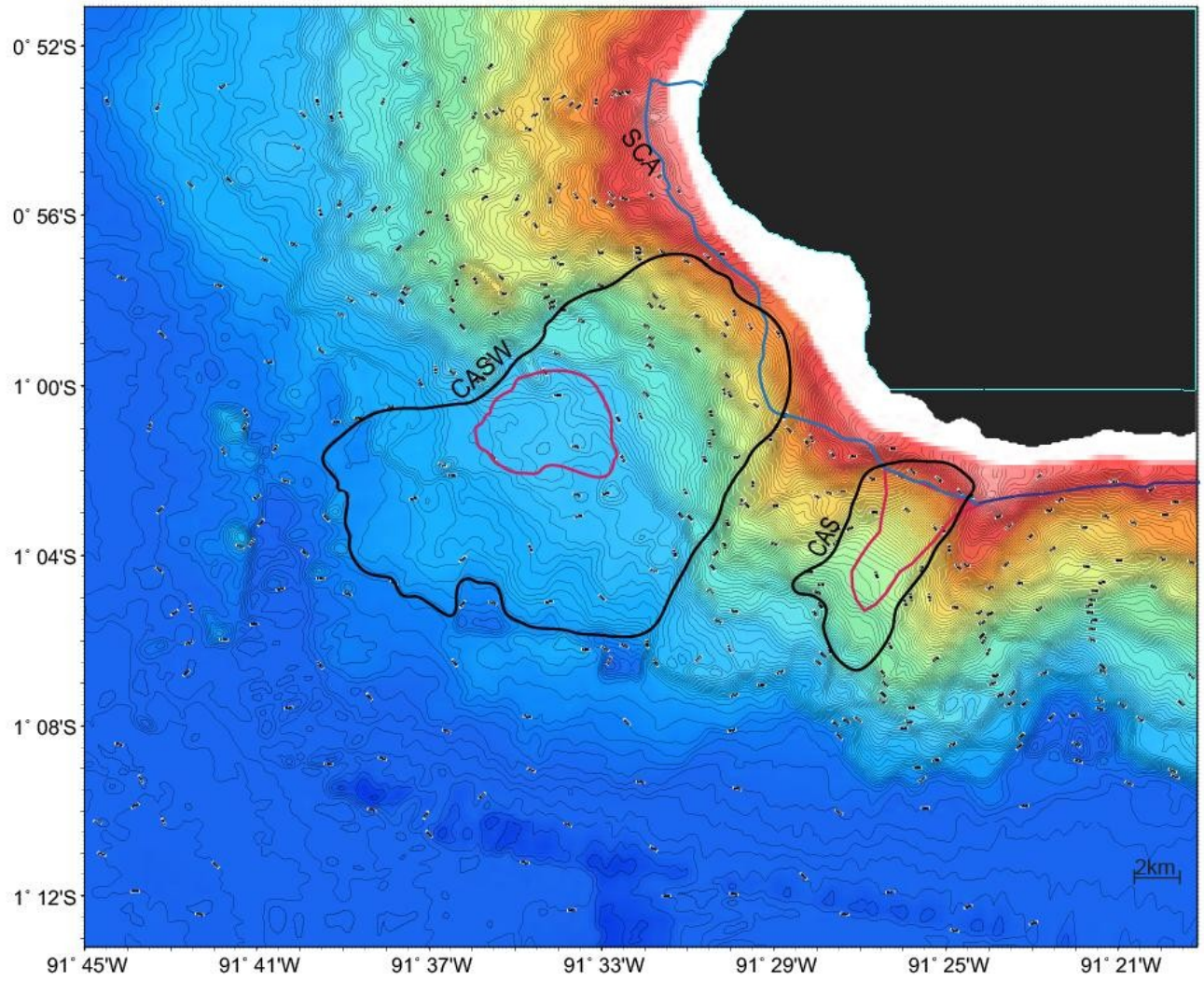

Figure 5. Cerro Azul bathymetry contours with interpretations. Contour interval is 25 meters. Interpretations are the same as in Figure 4.

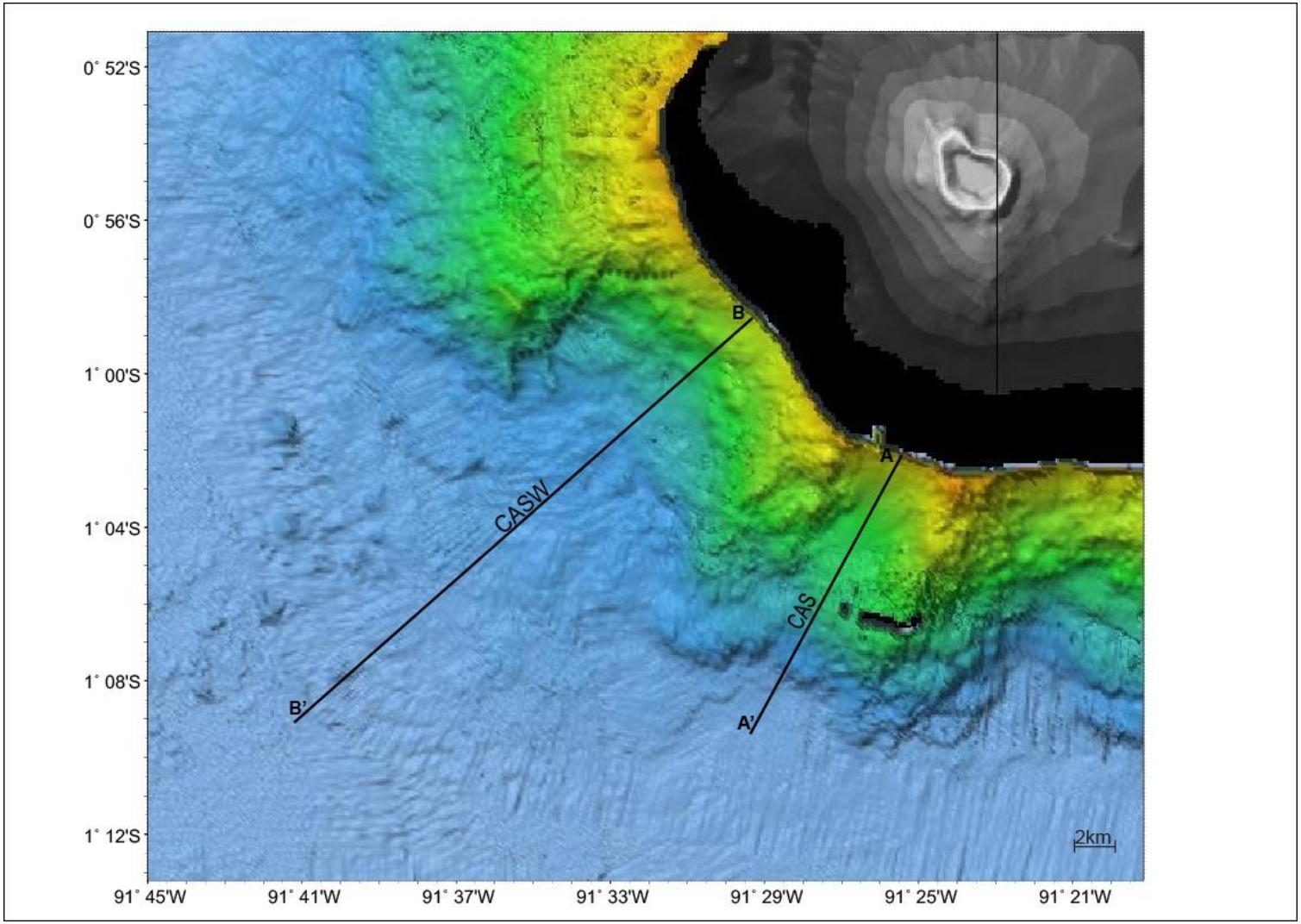

Figure 6. Cerro Azul shaded relief bathymetry map. Indicates the locations of scarps and lines show locations of depth cross section profiles A to A' and B to B', which are shown in Figure 7.

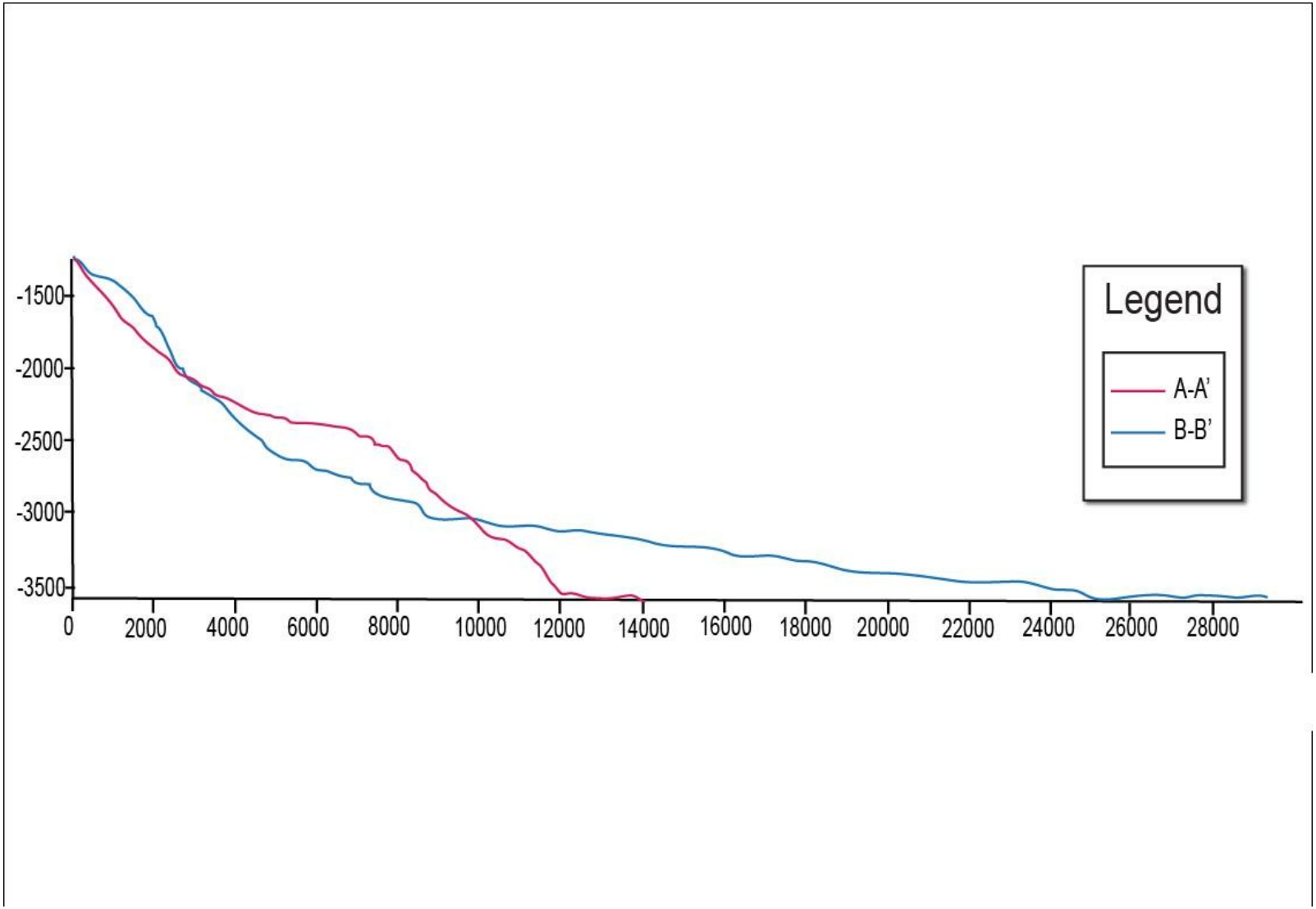

Figure 7. Cerro Azul depth profiles. Locations shown in Figure 6.

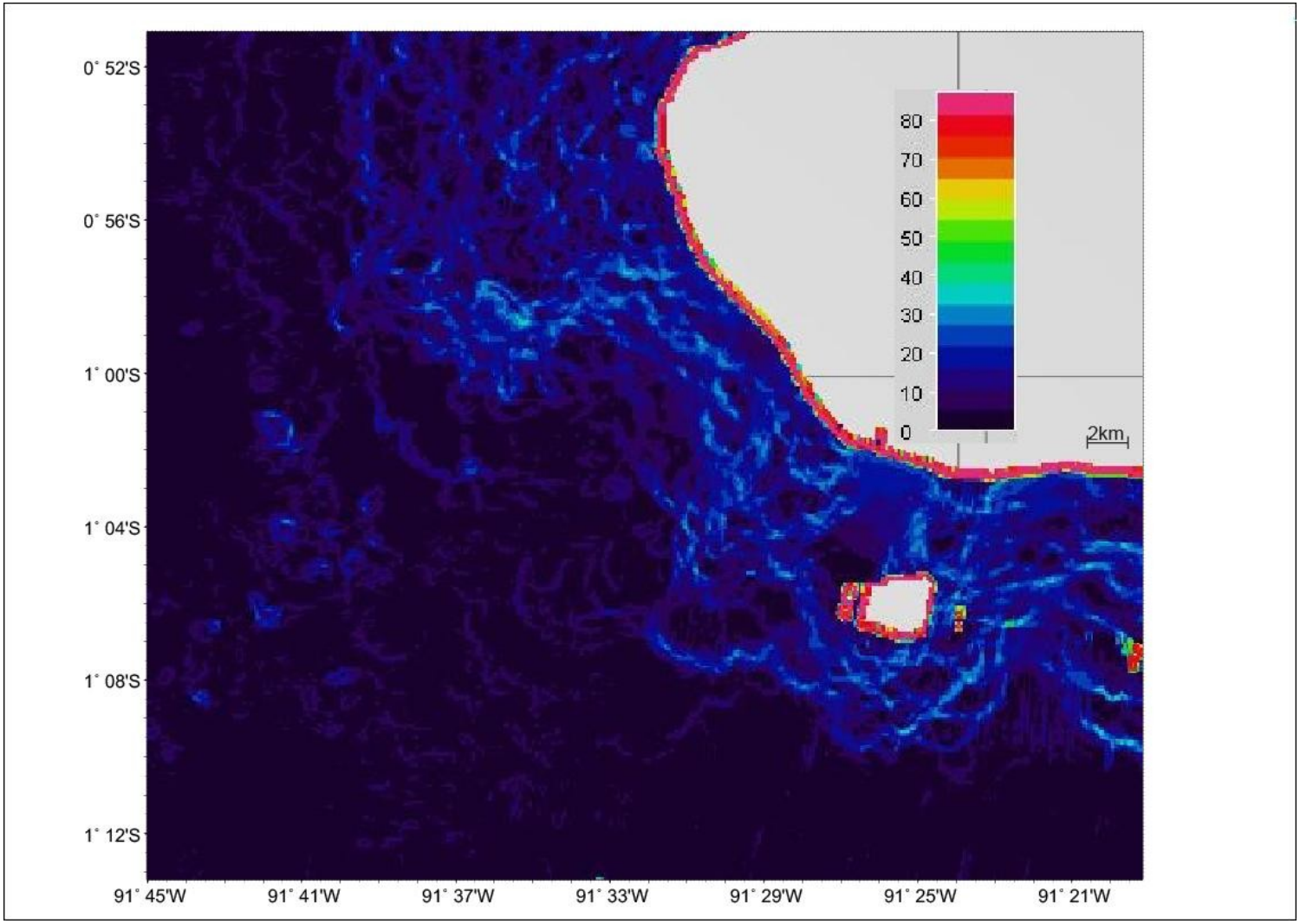

Figure 8. Cerro Azul slope angle map. Colors are indicative of average slope angle, with lighter colors representing steeper slopes.

3.1 Cerro Azul Region

The Cerro Azul region contains one slump, SCA, and two debris flows, CAS and CASW. The slump lies on the steep upper slopes of Isabela Island and can only be identified in the sidescan sonar image (Figure 4). The slump sheet is identified as having moderate backscatter amplitude with folds that give the impression of a rippled appearance in sidescan sonar images. The slump has a length of 33.1 km and a width of 1.8 km. The area of this slump in the sidescan sonar data is 55.4 km^2.

Both CAS and CASW debris flows can be differentiated in both the sidescan sonar and the bathymetry (Figure 5) are located between rift zone ridges and exist in large horseshoe shaped embayments (Figures 4 & 5). Both slide areas defined by sidescan sonar exist within the bounds of the bathymetry interpretations, but are significantly smaller in area.

CAS is located off the southernmost tip of Isabela Island and terminates in water depth of approximately 2700 meters. In the sidescan sonar data, this slide is identified with downslope lineations and extends for 7.2 km from the base of the slump sheets, has a maximum width of 4.6 km and an area of 17.5 km^2. Based on the bathymetry this slide features extends 10.6 km from the base of the slump sheet, has a maximum width of 5.1 km and an area of 44.9 km^2. The shaded relief bathymetry map, Figure 6, illuminates an area of steeper, rough slope on the northwest valley wall. The depth profile A to A' (Figure 7) indicates that there is a general concave upward trend in the upper slope with a decrease in slope with increased water depth and a hummocky bulge that begins at ~2200 meters depth, indicating a displaced mass on the lower slope. The slope angle

map shows that the slide is located in an amphitheatre shaped valley where the edges of the slide and the surrounding rift zone has a higher slope of ~30 degrees whereas the amphitheatre floor has a lower slope angle of ~10-20 degrees which decreases to nearly zero off the platform (Figure 8). This slide appears to have a combined source of subaerial and submarine, originating from both the two small subaerial horseshoe embayments, as well as the embayment on the upper submarine slopes.

CASW is located to the west of CAS and continues off the platform to terminate in water depths of ~3375 meters. In the sidescan sonar data, this slide is identified by a mottled and streaky appearance and exists off the platform. It has a length of 6.4 km, a width of 4.7 and an area of 21.3 km^2. The bathymetry shows that this slide extends from the base of the slump sheet for a distance of 19.8 km, has a maximum width of 15.9 km and an area of 208.3 km^2. The shaded relief bathymetry map (Figure 6) shows steep, rough slopes that border the NW and SE edges of the slide canyon. The continuity of the steep, rough slopes on the NW side implies a scarp that borders this edge of slide. In Figure 7, profile B-B' shows that this slide has a general concave upward trend with a decrease in slope angle with increased water depth. A rough surface texture begins at ~3000 meters depth and continues to a depth of ~3600 meter, where there is a bulge indicating a debris toe on the seafloor. The concave upward slope trend from the upper slope changes to a linear slope at the base. It like the concave upward trend has been filled by a sediment sheet. The slope angle map defines the CASW slide valley with steeper slopes on the NW, N and SE sides and shallower slopes on the canyon floor (Figure 8). This slide is directly related to the subaerial embayment on the southwest tip

of Cerro Azul volcano. Based on bathymetric calculations, this slide is the largest in the western Galapagos Islands.

3.2 Le Cumbre Region

The Le Cumbre/Fernandina region contains two slumps, SLCW and SLCN and three debris flows, LCSW, LCNW and LCN. The slump sheets are located on the steep upper slopes of Fernandina Island, can only be identified in the sidescan sonar image (Figure 9) and have similar characteristics to slumps offshore of Cerro Azul. SLCW is on the west side of Fernandina, has a length of 17.7 km, width of 1.6 km, and area of 27.0 km^2. SLCN is on the north side of Fernandina Island, has a length of 19.5 km, width of 1.2 km and area of 93.7 km^2.

All three debris flows, LCSW, LCNW and LCN, can be differentiated in both the sidescan sonar and the bathymetry (Figure 10). The slide areas defined by sidescan sonar extend slightly beyond the bounds of the bathymetry interpretations, yet are still smaller in area.

LCSW is located off the west coast of Fernandina Island and ends in water depth of ~3000 meters. This debris flows is located between rift zone ridges. In the sidescan sonar data, this slide has downslope lineations which are interrupted by lava flows and volcanic cones. Based on sidescan sonar data, this slide extends for 10.5 km from the base of the slump sheets, has a maximum width of 4.0 km and an area of 27.6 km^2. Based on the bathymetry this slide feature extends to the base of the platform for 12.5 km and includes part of the area covered by the slump sheet. It has a maximum width of 5.0 km and an area of 66.9 km^2. The shaded relief bathymetry map (Figure 11)

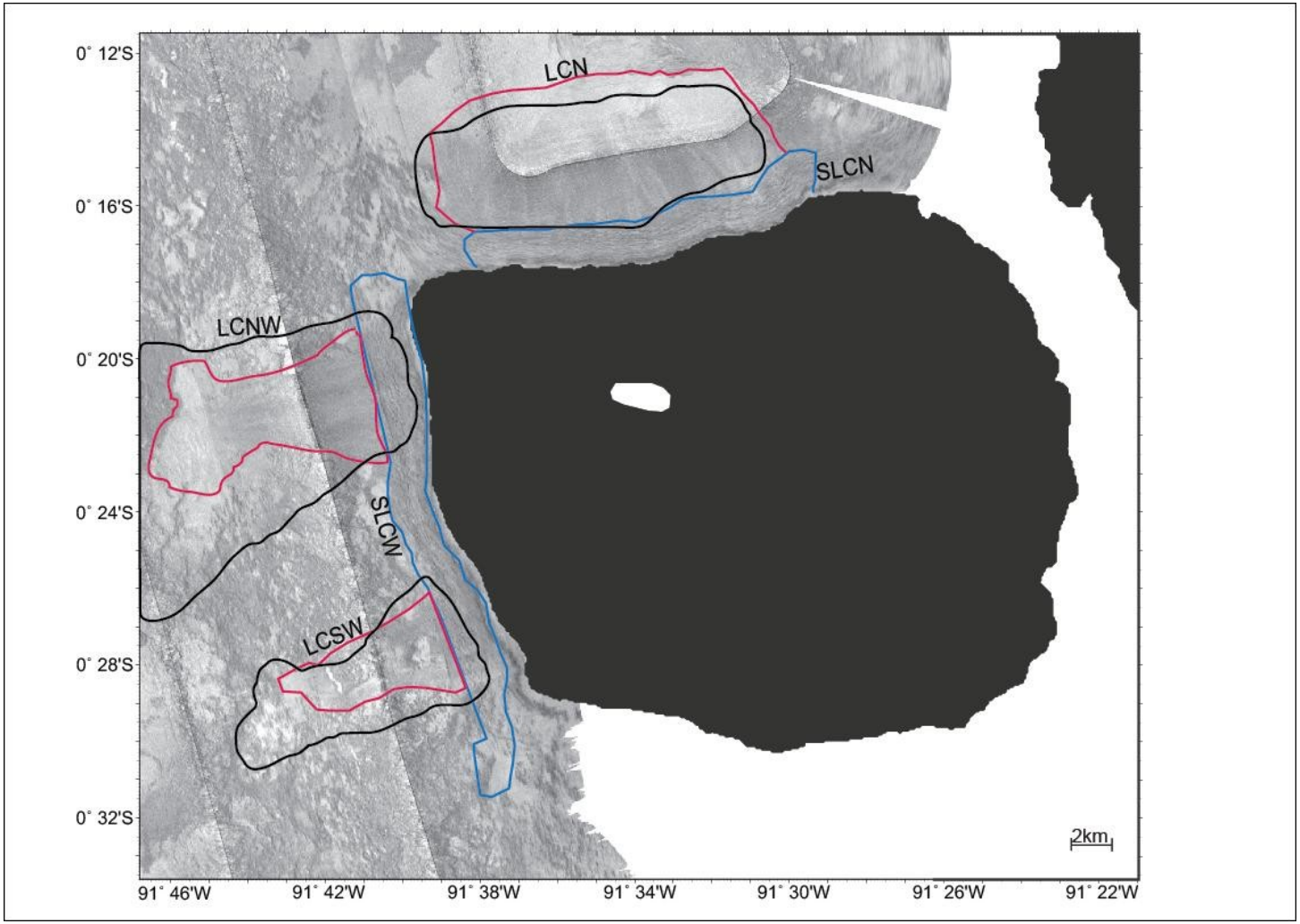

Figure 9. Le Cumbre sidescan sonar data interpreted. Interpretations include slump sheets outlined in blue and debris flows outlined in red with bathymetry interpretations outlined in black. Plot conventions as in Figure 4. Location shown in Figure 3.

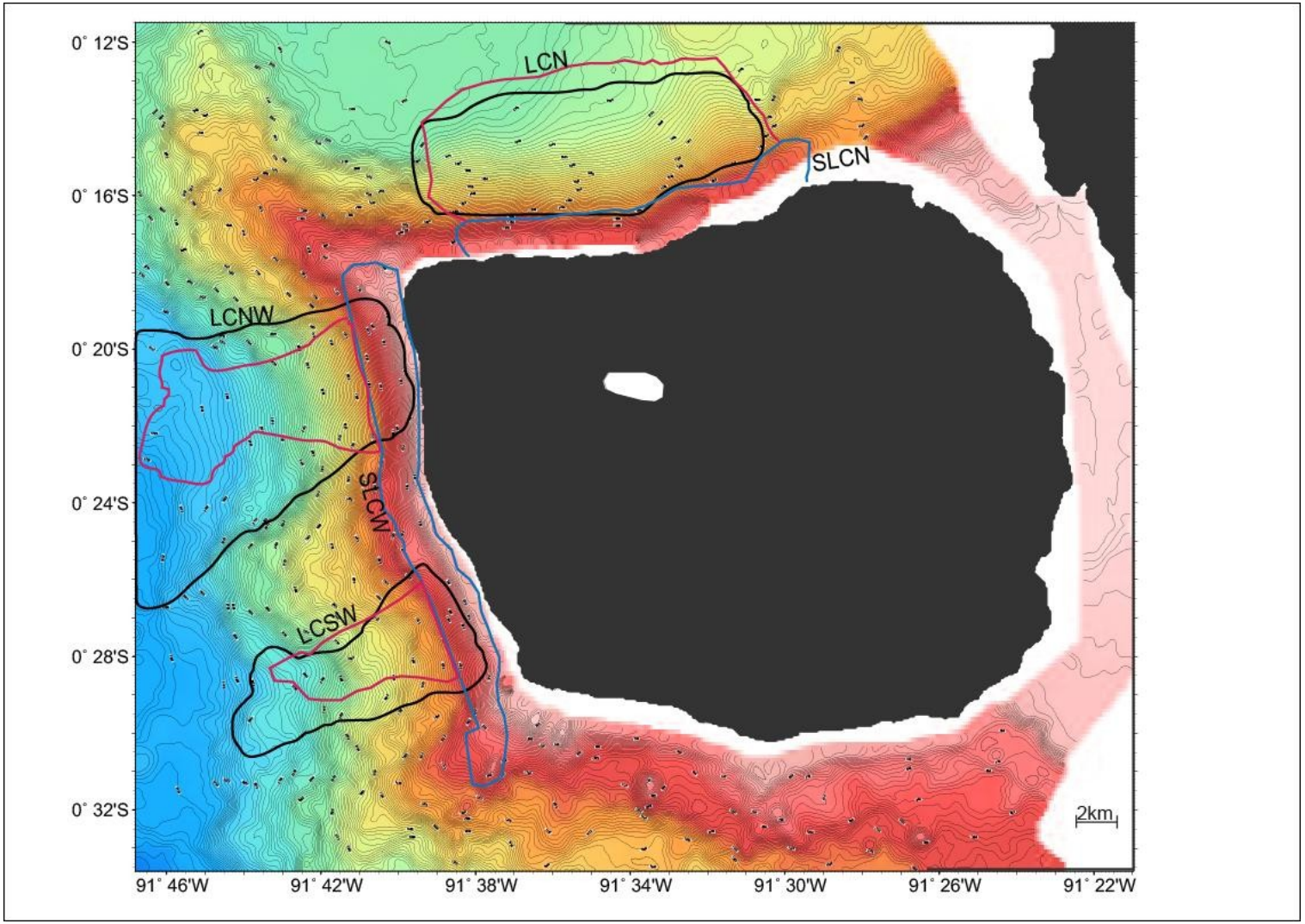

Figure 10. Le Cumbre bathymetry contours with interpretations. Contour interval is 25 meters. Interpretations are the same as in Figure 9.

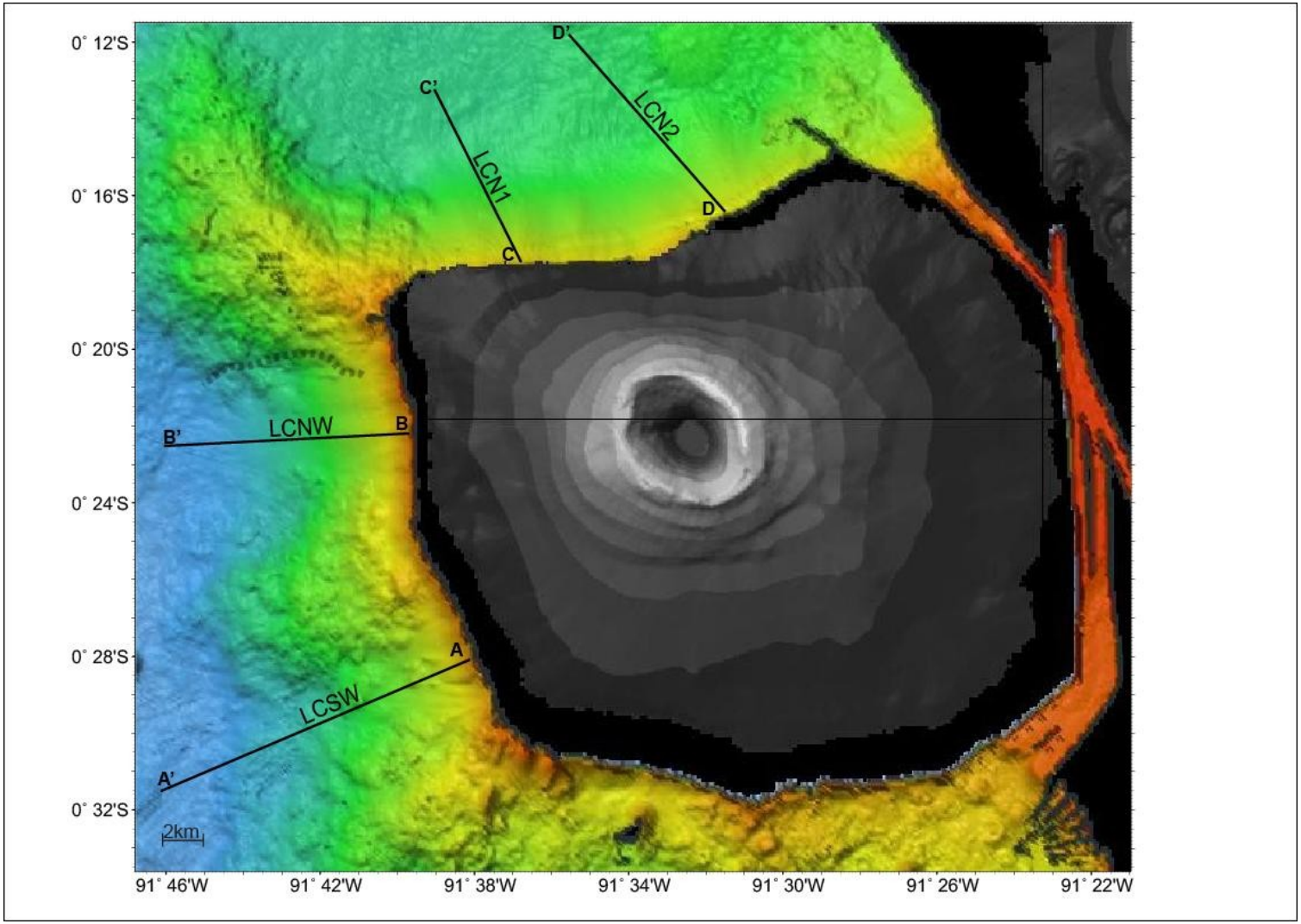

Figure 11. Le Cumbre shaded relief bathymetry map. Indicates the locations of scarps and lines show locations of depth cross section profiles A to A', B to B', C to C' and D to D', which are shown in Figure 12.

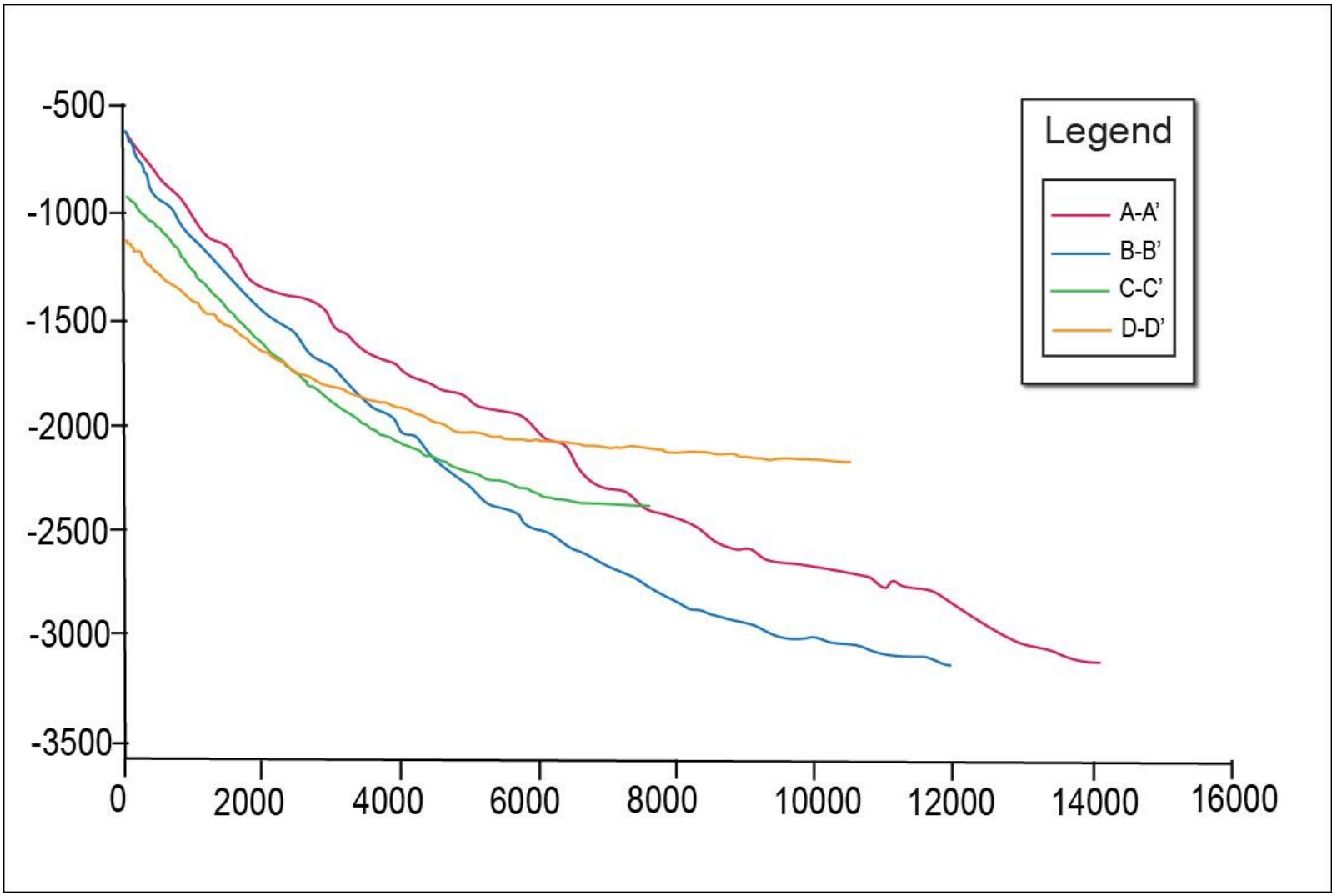

Figure 12. Le Cumbre depth profiles. Locations shown in Figure 11.

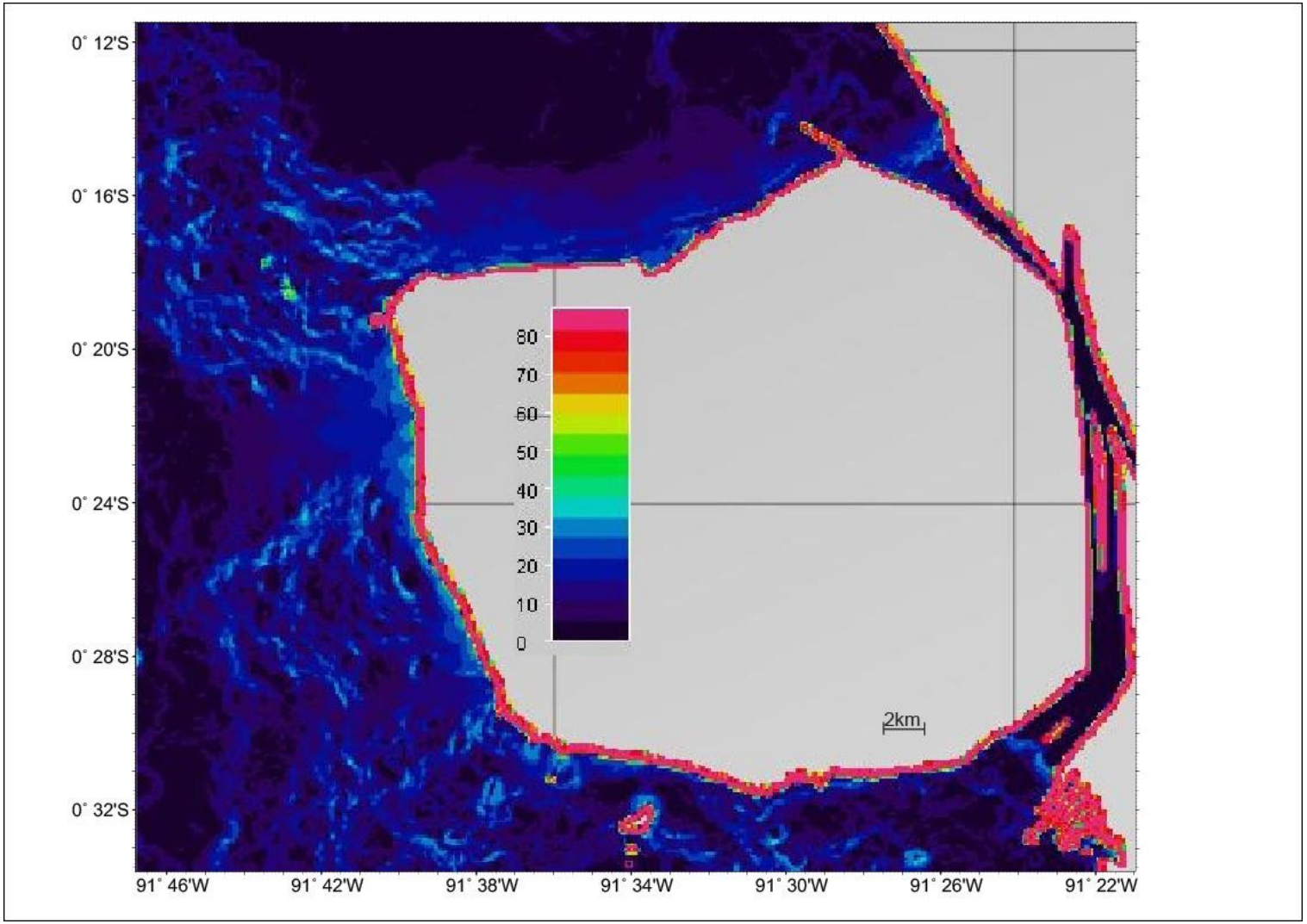

Figure 13. Le Cumbre slope angle map. Plot conventions as in Figure 8.

shows rough bathymetry of the rift zones that contrast with the smoother seafloor and horseshoe shape of the slide valley. The depth profile A to A' (Figure 12) indicates that there is a general concave upward trend in the slope with a decrease in slope angle with increased water depth. A bumpy texture begins at ~1100 meters depth and continues to the interpreted base of the slide indicating a series of discrete debris deposits. The slope angle map shows that the edges of the slide are not as clearly defined with sharp steep sides and the surrounding rift zone terrain has a higher slope of ~30 degrees compared to the lower angle of ~ 10-20 degrees in the slide area (Figure 13). This slide occurs in an isolated submarine embayment and has no apparent subaerial source.

LCNW is located off the west coast of Fernandina Island, north of LCSW and ends off the platform at a water depth of ~3275 meters. This debris flows is located between rift zone ridges. In the sidescan sonar data, this slide is indentified by downslope lineations and extends for 10.9 km from the base of the slump sheets, has a maximum width of 5.0 km and an area of 46.6 km^2. Based on the bathymetry this slide feature extends for 12.4 km and includes part of the area covered by the slump sheet. It has a maximum width of 11.4 km and an area of 166.2 km^2 as a minimum because the slide extends out of the data region The shaded relief bathymetry map (Figure 11) illuminates a scarp that bounds the northern edges of the slide, the horseshoe shaped embayment and the smooth bathymetry of the slide area. The depth profile B to B' (Figure 12) indicates that there is a general concave upward trend in the slope with a decrease in slope angle with increased water depth with a bumpy texture that begins at ~1500 meters depth and continues to the interpreted base of the slide. The slope angle

map sharply defines the slide's amphitheatre-shaped valley, by the contrast between the steep edges and the smooth bottom. The edges of the slide and the surrounding rift zone have a higher slope of ~30 degrees compared to ~25 degrees on the upper slopes, decreasing to ~10 degrees on the lower slope and nearing zero as the slide extends off the platform (Figure 13). This slide occurs in an isolated submarine embayment that has no apparent subaerial source.

LCN is located off the north coast of Fernandina Island and ends in water depth of ~2375 meters. In the sidescan sonar data, this slide is identified by downslope lineations and extends for 6.7 km from the base of the slump sheets, has a maximum width of 15.0 km and an area of 112.0 km^2. Based on the bathymetry this slide extends from the base of the slump sheets for 5.7 km, has a maximum width of 16.3 km and an area of 101.3 km^2. The shaded relief bathymetry map (Figure 11) highlights the smooth bathymetry of the slide area. The depth profiles C to C' and D to D' (Figure 12) indicate that there is a general concave upward trend in the slope with a flattening of the slope with increased depth. The slope angle map shows that the slide is located in a broad amphitheatre with steep upper slopes that near zero at depth (Figure 13). This slide occurs off the concave north coast of Fernandina, implying that the submarine slide feature is part of a larger collapse that shaped the north side of the volcano.

3.3 Volcan Ecuador Region

The Volcan Ecuador region contains two slump sheets, SVEW and SVEN, one debris flow which incorporates detached blocks, VEW, and two debris flows, VENW and VEN. The slumps can only be identified in the sidescan sonar image (Figure 14)

and have the same ropy fold characteristics as the Cerro Azul region. SVEW is located on the steep northwestern most tip of Isabela Island and has a length of 4.4 km, width of 2.1 km, and area of 13.6 km^2. SVEN is located on the steep upper north slope of Isabela Island, and has. It has a length of 28.1 km, width of 1.6 km and area of 56.4 km^2.

All three debris flows, VEW, VENW and VEN, can be differentiated in both the sidescan sonar and the bathymetry (Figure 15) and are located between rift zone ridges. The slide areas defined by bathymetry extend slightly beyond the bounds of the sidescan sonar interpretations and are larger in area.

VEW is located off the northwestern tip of Isabela Island and ends in water depth of ~2575 meters. In the sidescan sonar data, this slide has a mottled and streaky appearance which is interrupted by lava flows and volcanic cones. Within this slide the sonar image shows three detached blocks which can be identified by a margin of high backscatter amplitude, appearing dark in the images, with upper surfaces characterized by low backscatter amplitude, which appear white. Based on sidescan sonar data, this slide extends for 9.3 km from the base of the slump sheets, has a maximum width of 5.5 km and an area of 36.3 km^2. The detached blocks have an approximate length of 0.2 km. Based on the bathymetry this slide extends to the base of the platform for 11.0 km, has a maximum width of 7.3 km and an area of 68.2 km^2. The shaded relief bathymetry map (Figure 16) illuminates a steep, sharp, linear scarp that bounds the northernmost edge of the slide. This image also shows a horseshoe shaped embayment, a debris toe at the base of the slide and the smooth texture of the slide valley floor. The depth profile A to A' (Figure 17) indicates that there is a general concave upward trend in the slope with a

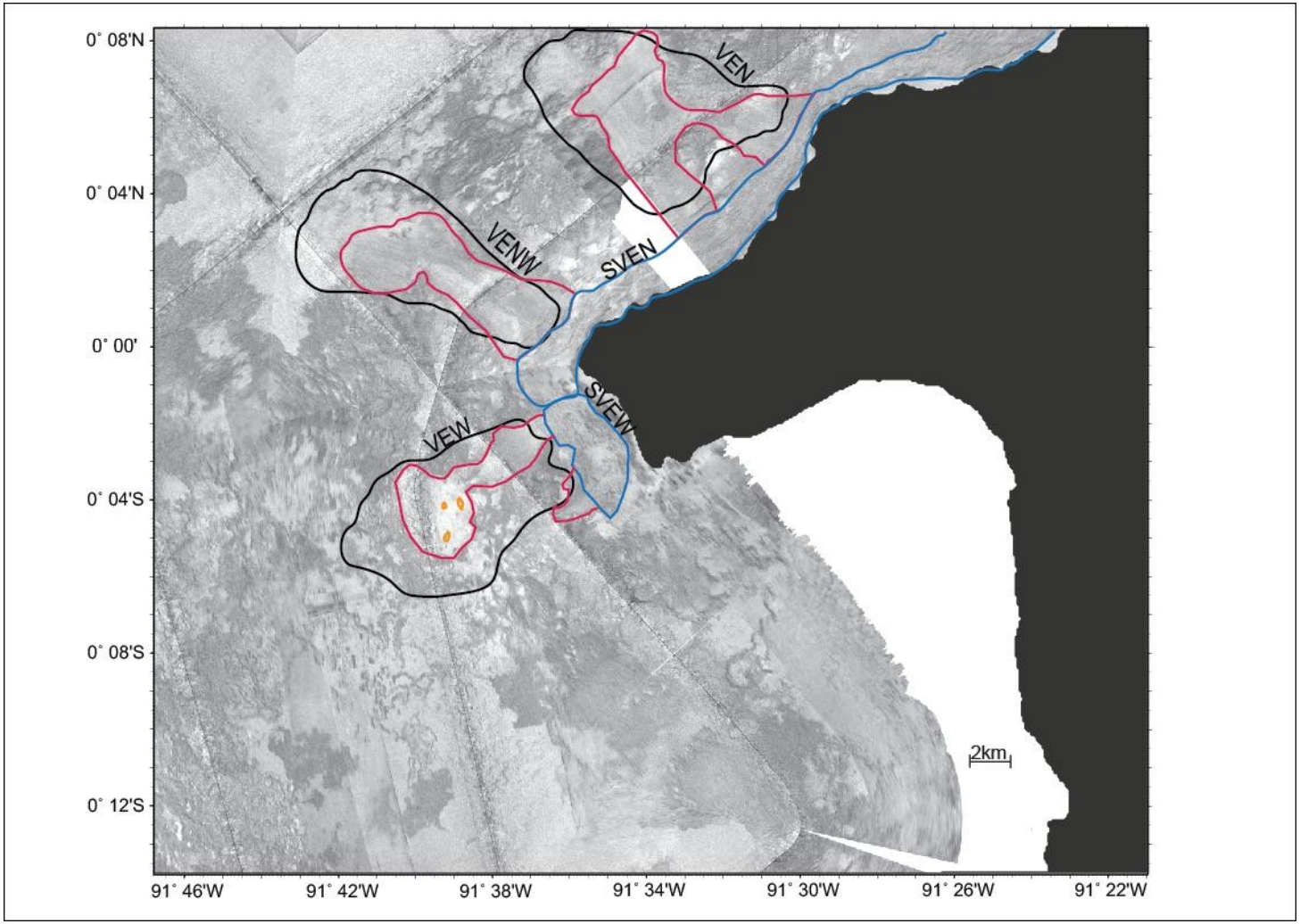

Figure 14. Volcan Ecuador sidescan sonar data interpreted. Interpretations include slump sheets outlined in blue, debris flows outlined in red, and detached blocks outlined in orange with bathymetry interpretations outlined in black. Plot conventions as in Figure 4. Locations shown in Figure 3.

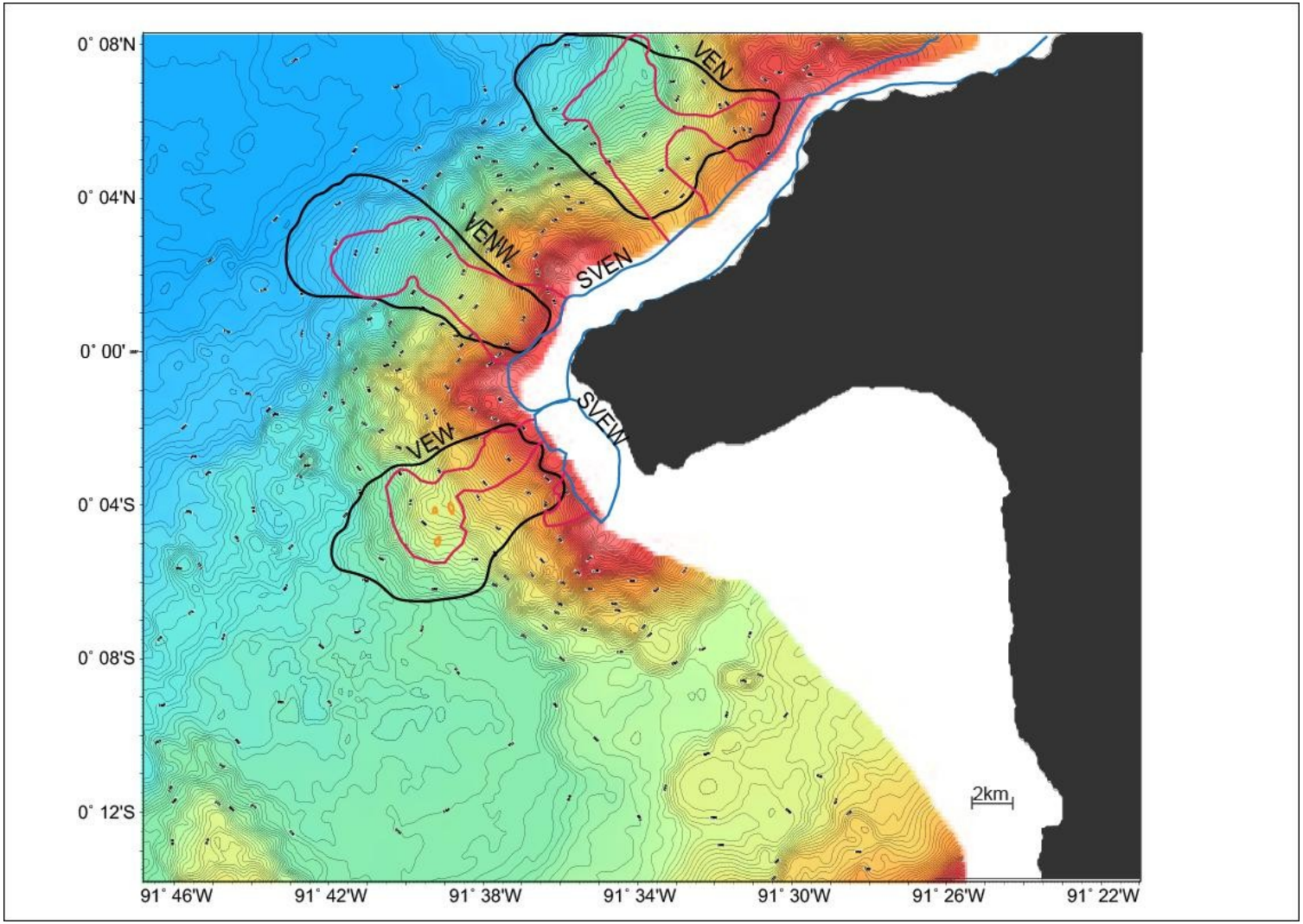

Figure 15. Volcan Ecuador bathymetry contours with interpretations. Contour interval is 25 meters. Interpretations are the same as in Figure 14.

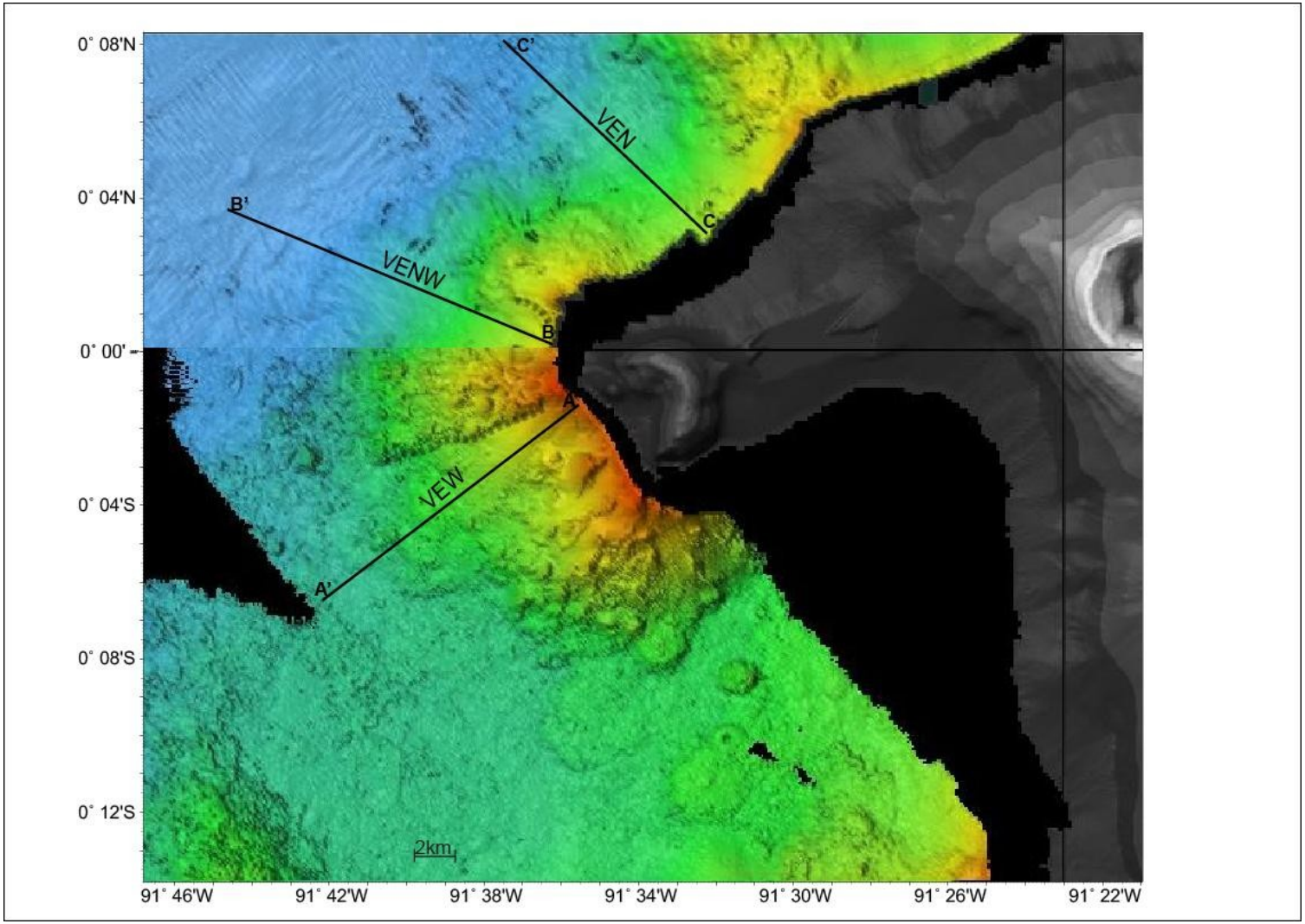

Figure 16. Volcan Ecuador shaded relief bathymetry map. Indicates the locations of scarps and lines show locations of depth cross section profiles A to A', B to B' and C to C', which are shown in Figure 17.

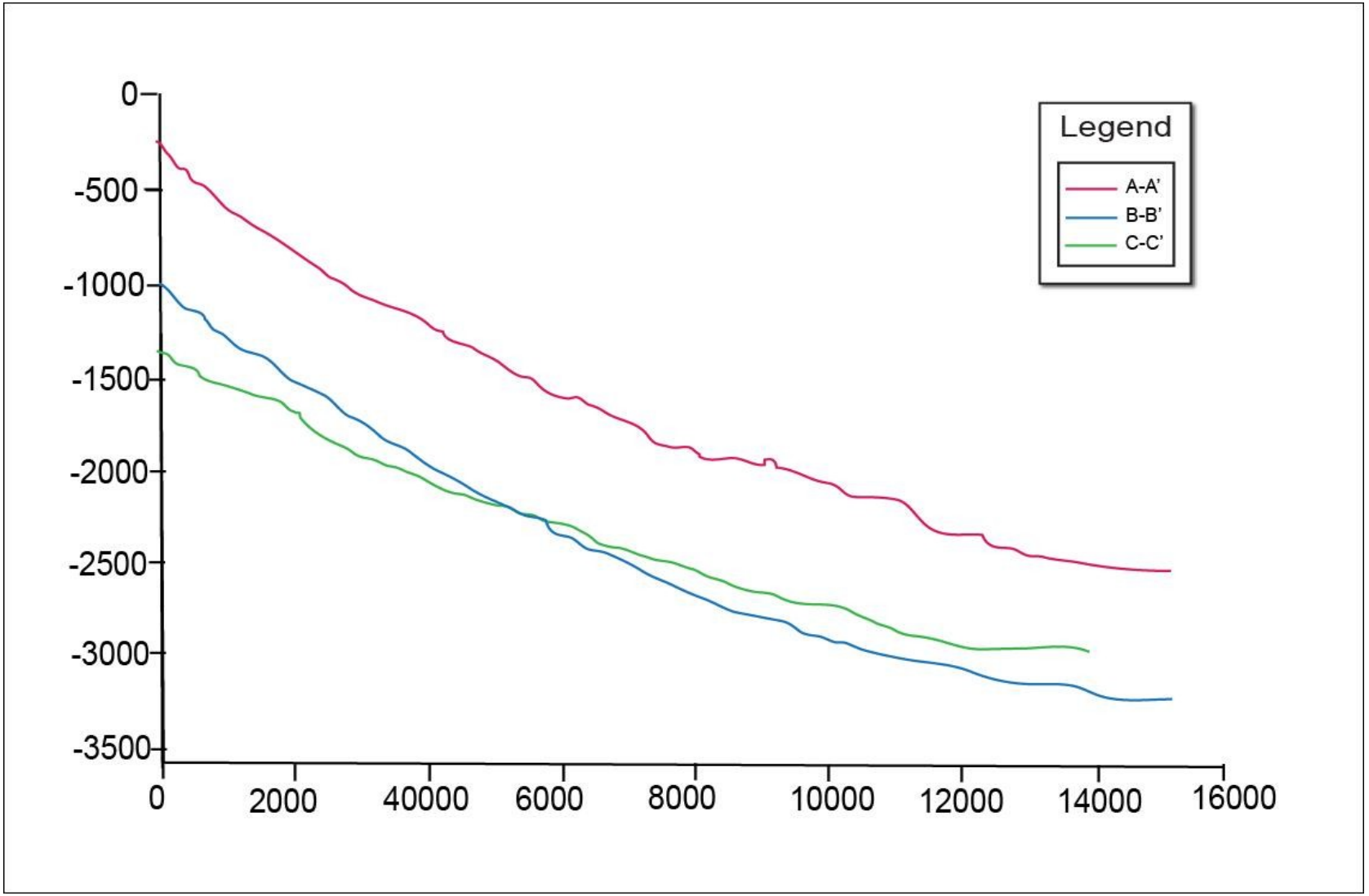

Figure 17. Volcan Ecuador depth profiles. Locations shown in Figure 16.

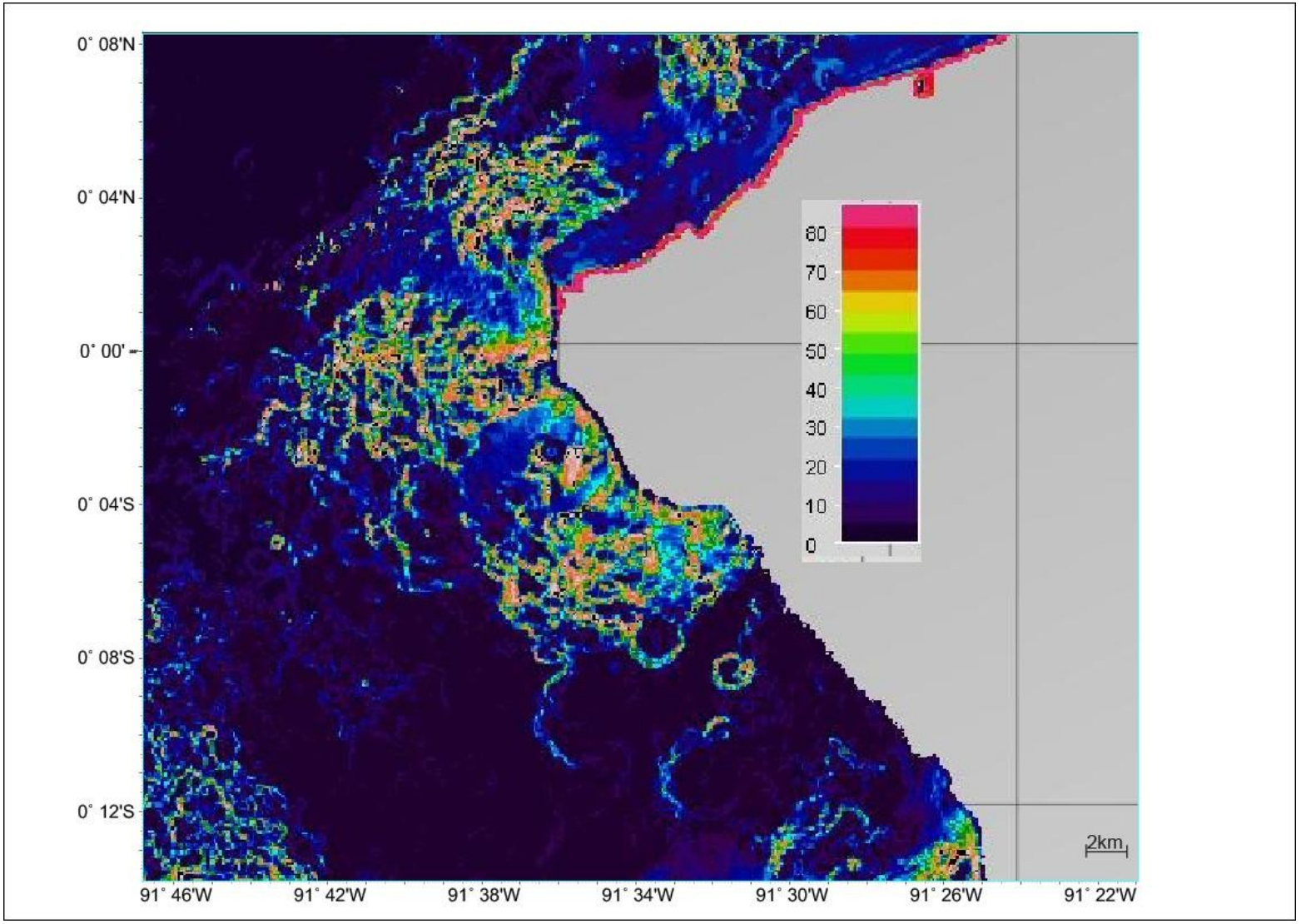

Figure 18. Volcan Ecuador slope angle map. Plot conventions as in Figure 8.

decrease in slope angle with increased water depth. A hummocky signature begins at ~1500 meters depth and continues to a depth of ~2250 meters. This profile also shows a bulge that begins at ~1900 meters depth and continues to the base of the slide, indicating the location of a debris toe. The slope angle map (Figure 18) defines the slide valley shape with steeper slopes on the sides and lower floor and shows a scarp on the north side and steep slopes on the southeast side. The map also shows several features on the lower floor that are part of the debris toe bulge. The edges of the slide, the surrounding rift zones, and the upper slope of the slide have a slope of >30 degrees, while the lower slope decrease from 25 to <10 degrees at the base of the slide. This slide is directly adjacent to the subaerial embayment and is associated with the collapse of Volcan Ecuador.

VENW is located off the northwestern tip of Isabela Island, north of VEW and ends off the platform at a water depth of ~3175 meters. In the sidescan sonar data, this slide is defined by downslope lineations and extends for 12.3 km from the base of the slump sheets, has a maximum width of 4.2 km and an area of 28.4 km^2. Based on the bathymetry this slide feature extends for 12.7 km from the base of the slump sheet, has a maximum width of 5.8 km and an area of 57.4 km^2. The shaded relief bathymetry map (Figure 16) illuminates a short scarp that bounds the upper northeastern edge of the slide area. These data also show the horseshoe shaped embayment and the smooth bathymetry of the slide valley floor. The depth profile B to B' (Figure 17) indicates that there is a general concave upward trend in the slope with a decrease in slope angle with increased water depth. The profile is generally smooth indicating a lack of large debris

deposits in the slide valley. The slope angle map shows that the slide has as similar signature to the VEW slide with several patches if high slope near the bottom of the slide valley that may represent debris piles (Figure 18). This slide occurs in an isolated submarine embayment and has no apparent subaerial source.

VEN is located off the north coast of Isabela Island and terminates at the base of the platform in water depth of ~3000 meters. In the sidescan sonar data, this slide is defined by downslope lineations and extends for 7.8 km from the base of the slump sheets, has a maximum width of 5.7 km and an area of 43.1 km^2. Based on the bathymetry this slide feature extends from below the slump sheets for 10.1 km, has a maximum width of 9.0 km and an area of 65.0 km^2. The shaded relief bathymetry map (Figure 16) illuminates a broad smooth valley for the slide area. The depth profile C to C' (Figure 17) indicates that there is a general concave upward trend in the slope with a flattening of the slope with increased depth. The smooth slope indicates only little debris piles on the slope. The slope angle map shows that the slide is located in an amphitheatre valley with shallow slopes less than 20 degrees that near zero in deep water (Figure 18). This slide occurs in an isolated submarine embayment and has no apparent subaerial source.

3.4 Roca Redonda Region

The Roca Redonda Region contains four debris flows, RRSW, RRNW, RRNE, and RRSE. No slumps were found in this region. Three debris flows, RRSW, RRNW, and RRNE can be differentiated in both the sidescan sonar and the bathymetry data, identified with downslope lineations in the sidescan sonar (Figure 19) and by concave

contours on the upper slopes and a fanning of the contours (convex contours) on the seafloor off the platform in the bathymetry data (Figure 20). RRSE can only be identified in the bathymetry data by the same characteristics as the other three slides. All four flows are located between rift zone ridges. The slide areas defined by sidescan sonar are smaller in area than the areas defined by bathymetry because they are narrower. The shaded relief bathymetry map (Figure 21) illuminates the smooth bathymetry of the horseshoe shaped embayments that each slide exists within. The depth profiles (Figure 22) indicate that there is a general concave upward trend in the slope with a decrease in slope angle with increased water depth. The slope angle map shows the amphitheatre like valley that the slide exists in and shows that the edges of the slide and the surrounding rift zone have a higher slope of ~30 degrees compared to the lower angle of ~ 10 degrees in the slide valley floor (Figure 23). The source of all four slides appears to be a combination of a subaerial sources associated with the steep cliff faces of Roca Redonda Island as well as the submarine embayments of each slides' respective upper slope.

RRSW is located off the southwest tip of Roca Redonda Island, just north of Isabela Island and terminates in water depth of ~3225 meters. Based on sidescan sonar data, this slide extends for 14.3 km from the island, has a maximum width of 6.8 km and an area of 68.4 km^2. Based on the bathymetry this slide extends 16.4 km, has a maximum width of 10.0 km and an area of 120.8 km^2.

RRNW is located off the northwest tip of Roca Redonda Island, north of RRSW and ends off the platform at a water depth of ~ 3075 meters. Based on sidescan sonar

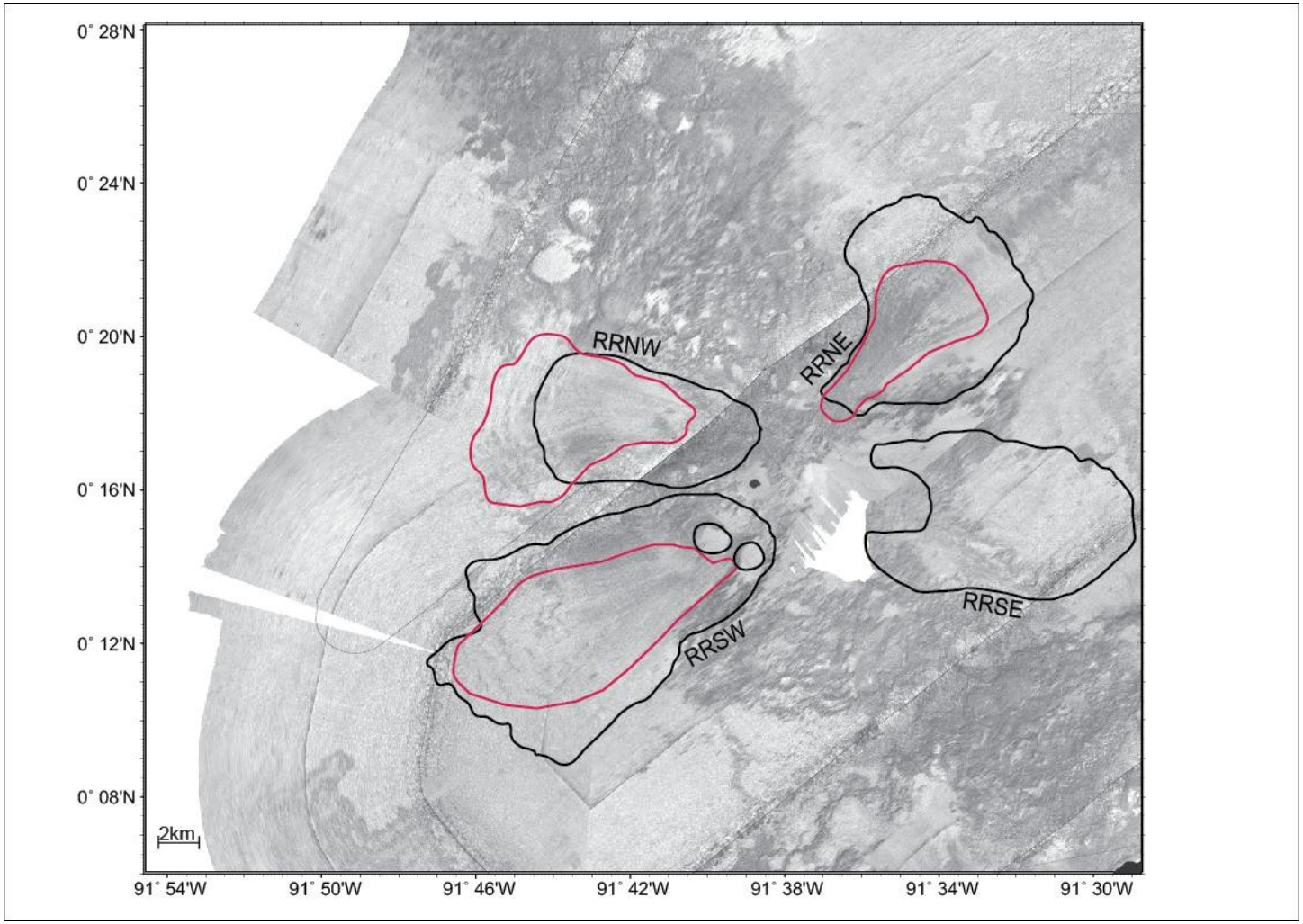

Figure 19. Roca Redonda sidescan sonar data interpreted. The area surrounding Roca Redonda Island north of Isabela Island. Interpretations include debris flows outlined in red with bathymetry interpretations outlined in black. Plot conventions as in Figure 4. Locations shown in Figure 3.

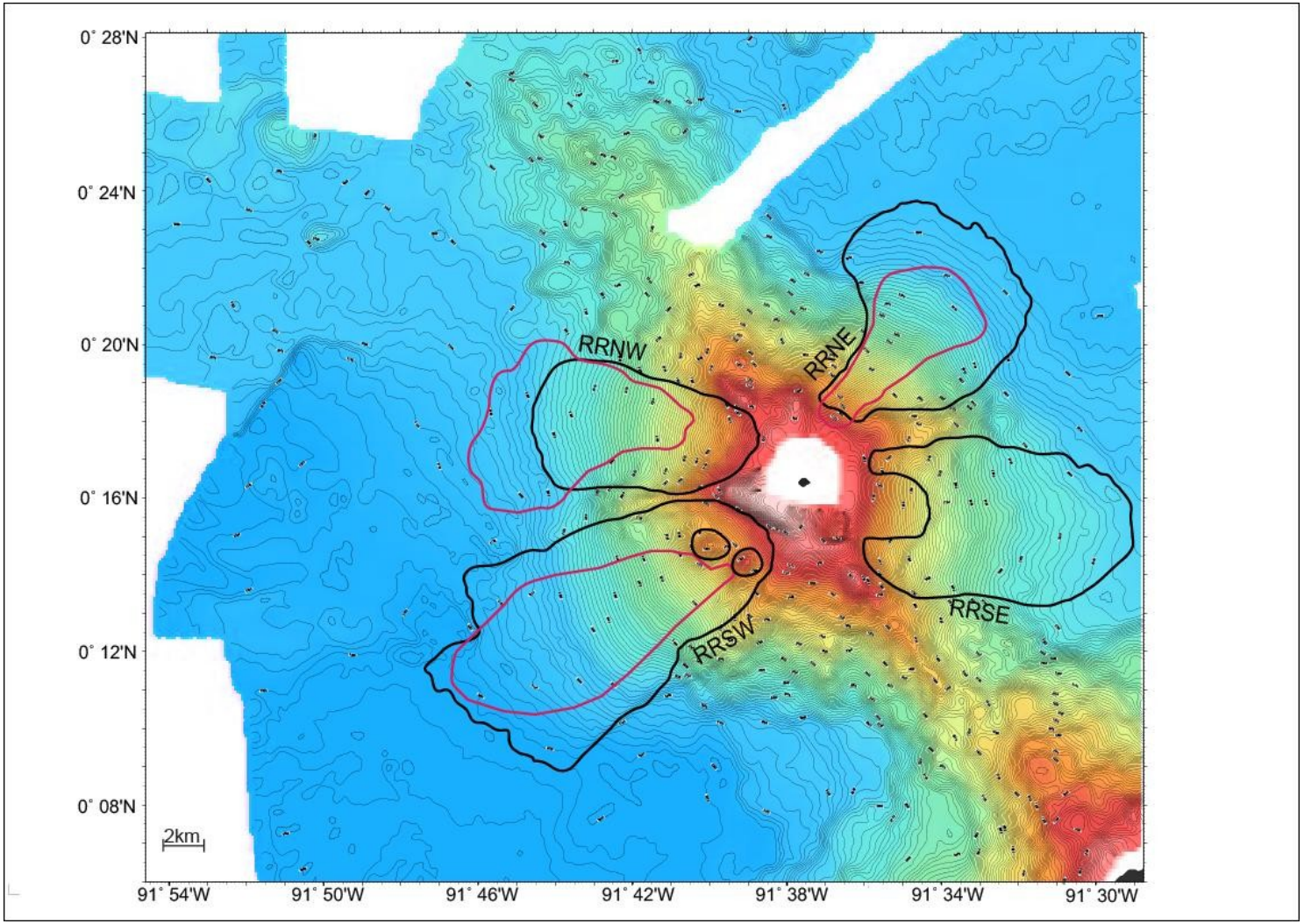

Figure 20. Roca Redonda bathymetry contours with interpretations. The area surrounding Roca Redonda Island north of Isabela Island. Contour interval is 25 meters. Plot conventions as in Figure 19.

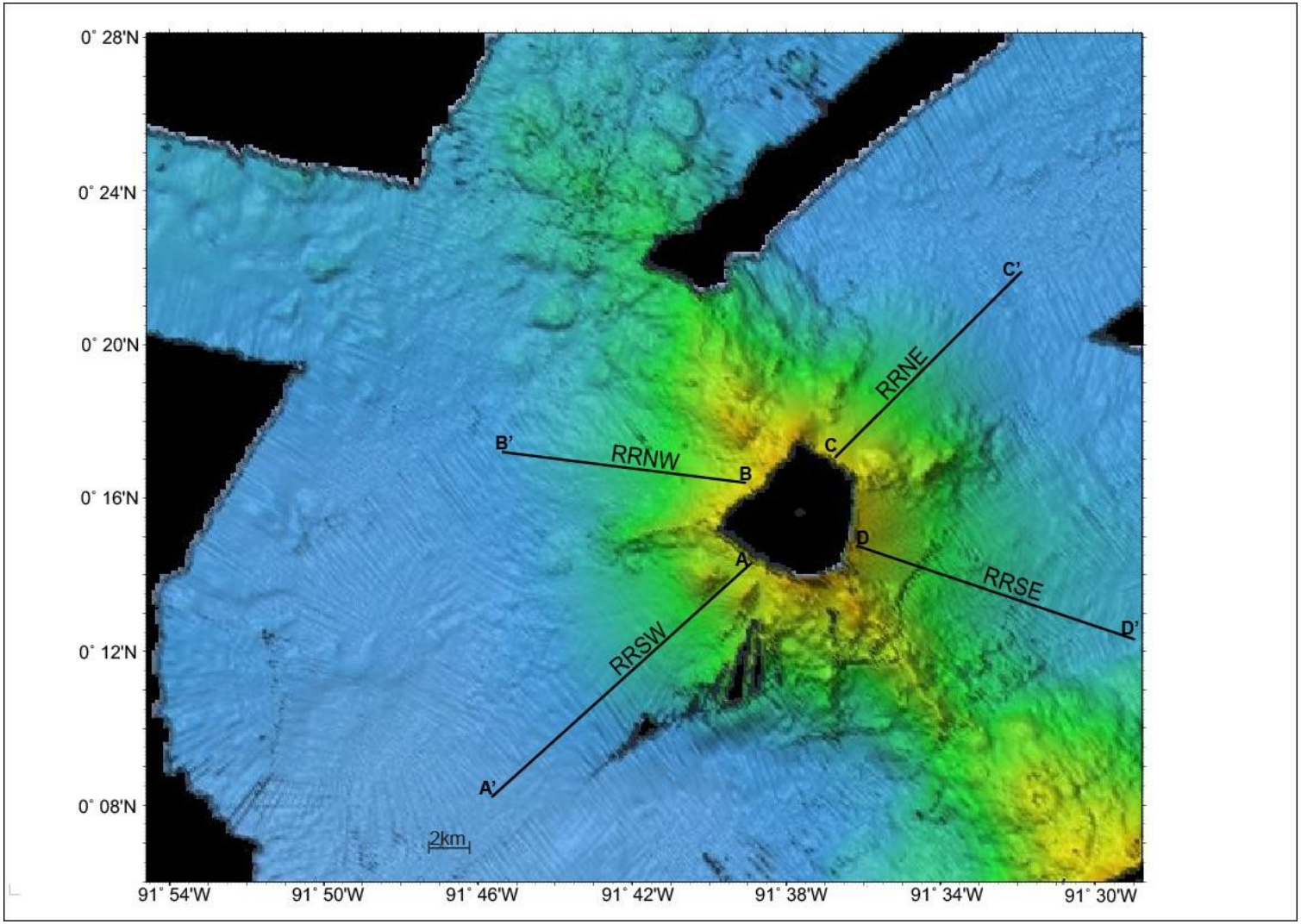

Figure 21. Roca Redonda shaded relief bathymetry map. Indicates the locations of scarps and cross section profiles A to A' in the southwest, B to B' in the northwest, C to C' in the northeast and D to D' in the southeast.

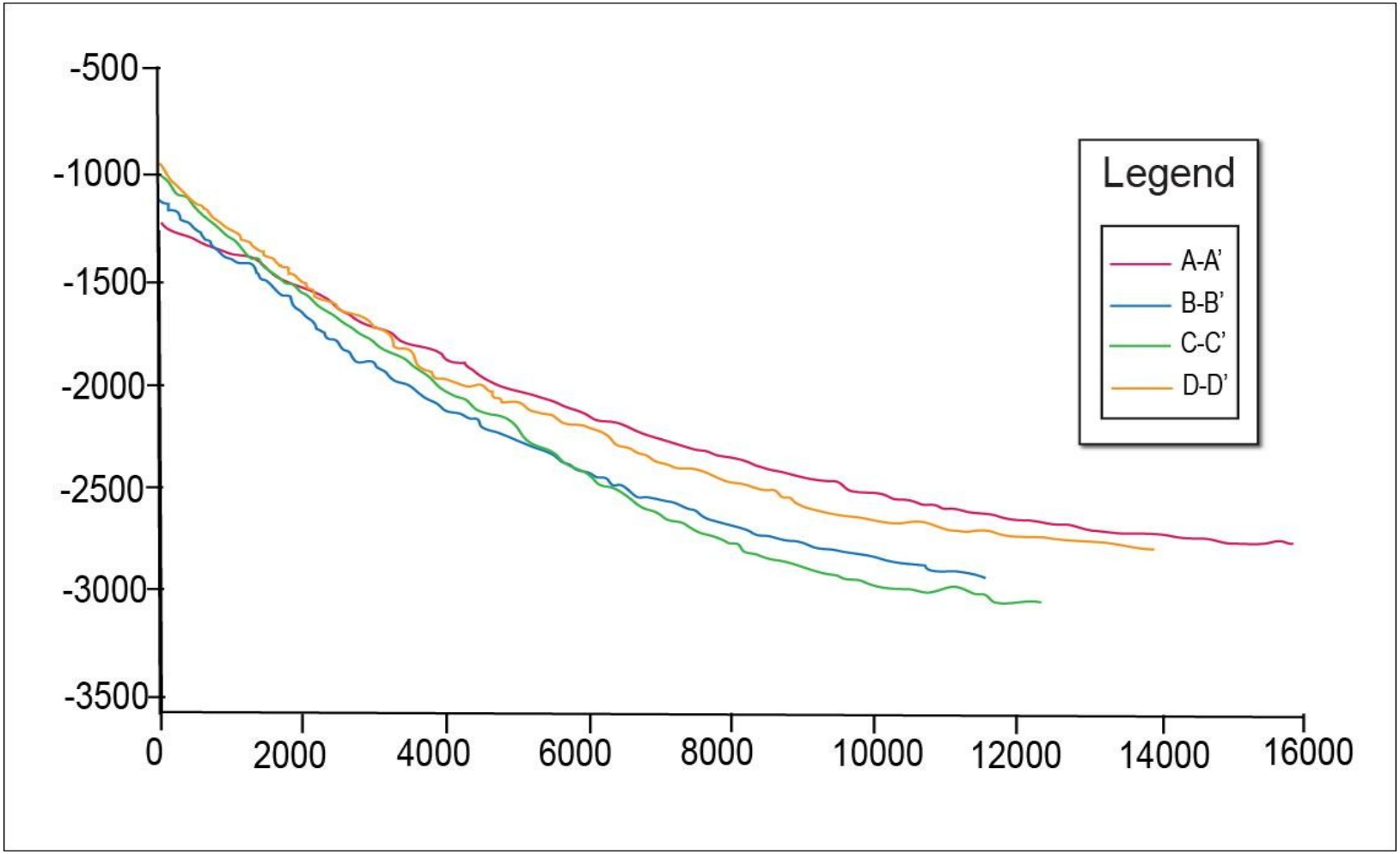

Figure 22. Roca Redonda depth profiles. Profile A to A' in red, B to B' in blue, C to C' in green and D to D' in orange show a general concave upward trend in the slope of the slide. Profile C to C' has a hummocky texture that begins at ~2100 meters and continues to the base of the slide and a bulge that can be seen at ~2950 meters indicating a displaced mass. Profile D to D' shows a headwall scarp located at ~1800 meters depth.

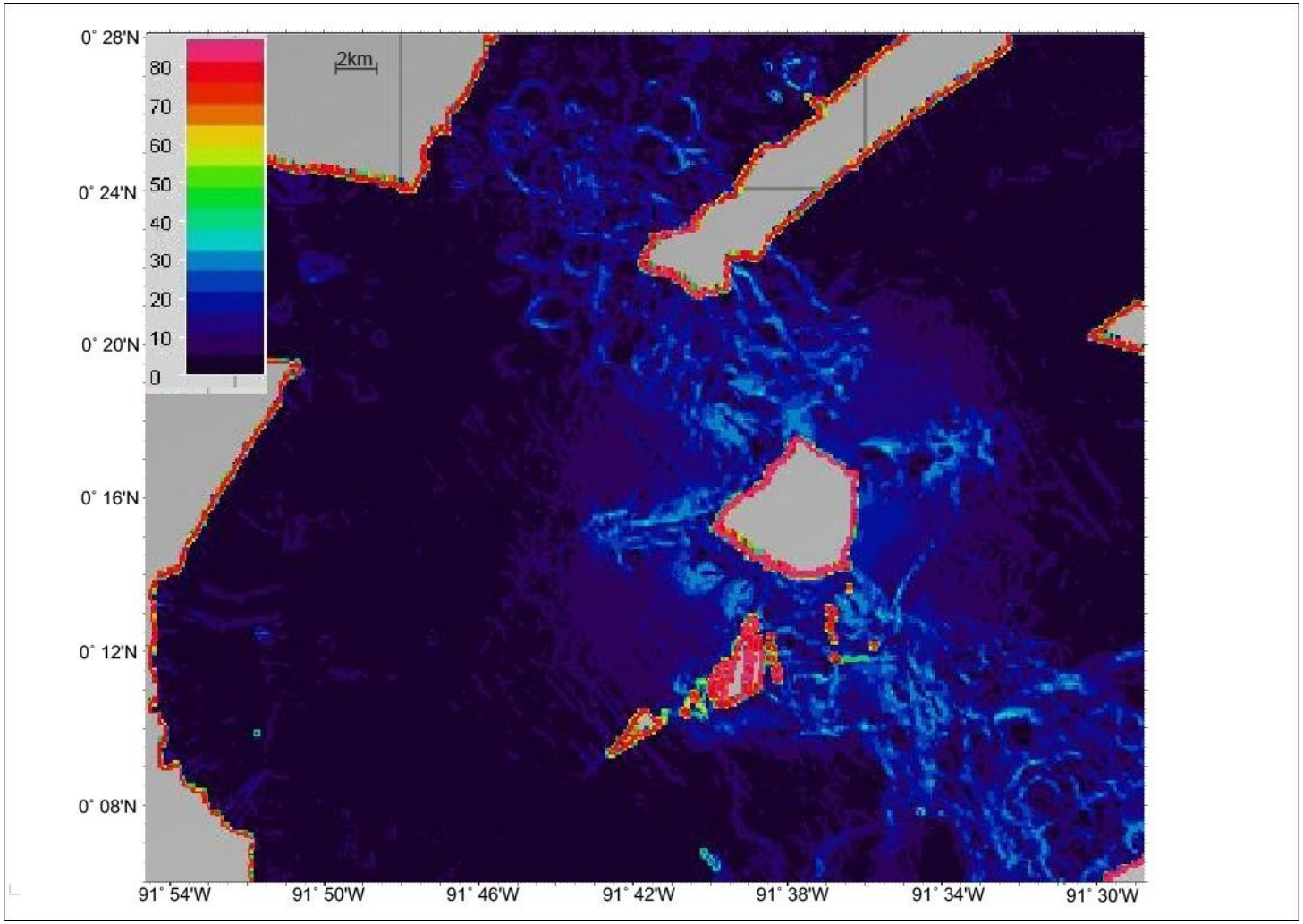

Figure 23. Roca Redonda slope angle map. The slope angle map shows the amphitheatre like valley that the slide exists in and shows that the edges of the slide and the surrounding rift zone have a higher slope of ~30 degrees compared to the lower angle of ~ 10 degrees in the slide area.

data, this slide extends for 13.0 km from the base of the slump sheets, has a maximum width of 6.9 km and an area of 61.0 km^2. Based on the bathymetry this slide extends for 11.3 km, has a maximum width of 5.8 km and an area of 57.4 km^2.

RRNE is located off the northeast tip of Roca Redonda Island, just north of Isabela Island and ends in water depth of ~ 3050 meters. Based on sidescan sonar data, this slide extends for 11.0 km, has a maximum width of 6.2 km and an area of 32.7 km^2. Based on the bathymetry this slide extends 12.7 km, has a maximum width of 10.4 km and an area of 77.1 km^2. The depth profile C to C' (Figure 22) indicates that the slope of the slide has a hummocky texture that begins at ~2100 meters and continues to the base of the slide. The profile also shows a bulge that can be seen at ~2950 meters which indicates a displaced mass.

RRSE is located off the southeast tip of Roca Redonda Island and ends in water depth of ~ 2850 meters. Based on the bathymetry this slide extends 13.9 km, has a maximum width of 7.9 km and an area of 81.04 km^2. A scarp, ~150 meters high can be identified in the bathymetry (Figure 20), the shaded relief bathymetry map (Figure 21), Profile D to D' (Figure 22), and in the slope angle map (Figure 23).

3.5 Volcan Wolf Region

The Volcan Wolf region contains two slump sheets, SVWN ad SVWE, and two debris flows, VWN and VWE. The slump sheets are located on the steep upper slopes of Isabela Island, can only be identified in the sidescan sonar image and have the same characteristics as the slumps off of Cerro Azul (Figure 24). SVWN is on the north side

of Isabela, has a length of 36.3 km, width of 2.3 km, and area of 86.3 km^2. SVWN is on the east side of Isabela, has a length of 7.06 km, width of 2.5 km and area of 33.9 km^2.

Both debris flows, VWN and VWE, can be identified in both the sidescan sonar and the bathymetry data. They are identified with downslope lineations in the sidescan sonar (Figure 24) and by concave contours on the upper slopes and a fanning of the contours (convex contours) on the seafloor at the base of the slope in the bathymetry data (Figure 25) and are located between rift zone ridges.

VWN is located off the north coast of Isabela Island and ends in water depth of ~3000 meters. This debris flow is located between rift zone ridges. Based on sidescan sonar data, this slide extends for 13.2 km from the base of the slump sheets, has a maximum width of 10.2 km and an area of 91.6 km^2. Based on the bathymetry this slide extends to the base of the platform for 10.4 km, has a maximum width of 9.2 km and an area of 88.4 km^2.

The shaded relief bathymetry map (Figure 26) illuminates a scarp that borders the eastern side of the slide, the horseshoe shaped embayment of the slide, and indicates that the lower slope has a hummocky texture which can also be seen in depth profile A to A' (Figure 27). In contrast, the upper slopes have a smooth bathymetry, which can be seen in depth profile B to B'. The depth profiles A to A' and B to B' (Figure 27) indicate that there is a general concave upward trend in the slope with a shallowing of the slope with increased depth with a hummocky structure that begins at ~2150 meters depth and continues to the interpreted base of the slide. Profile A to A' shows a bulge at ~2400 meters and continues to the base of the slide, indicating a debris toe at the base of

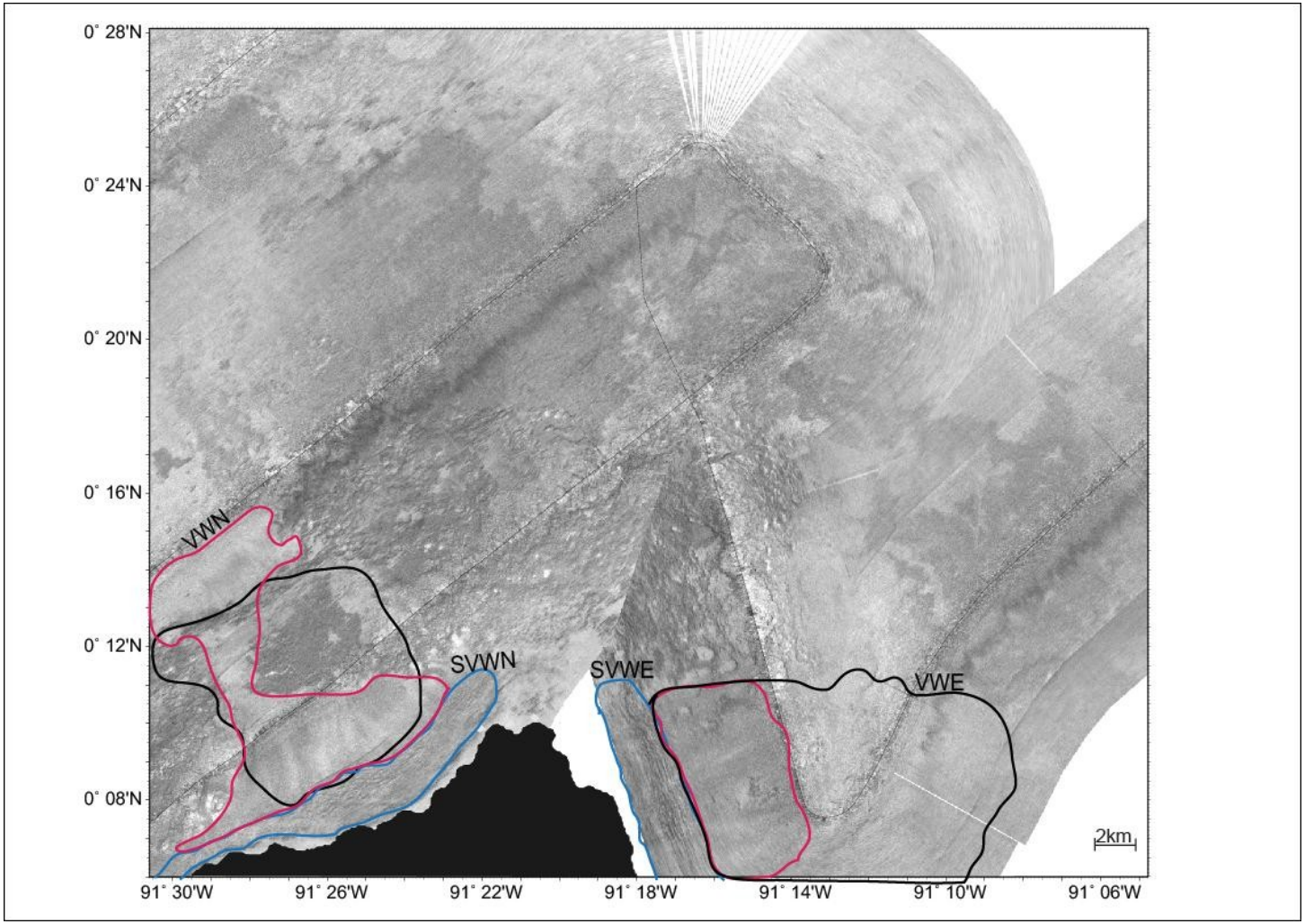

Figure 24. Volcan Wolf sidescan sonar data interpreted. The area off the coast of Volcan Wolf on the northeastern tip of Isabela Island. Interpretations include slump sheets outlined in blue and debris flows outlined in red, with bathymetry interpretations outlined in black. Plot conventions as in Figure 4. Locations shown in Figure 3.

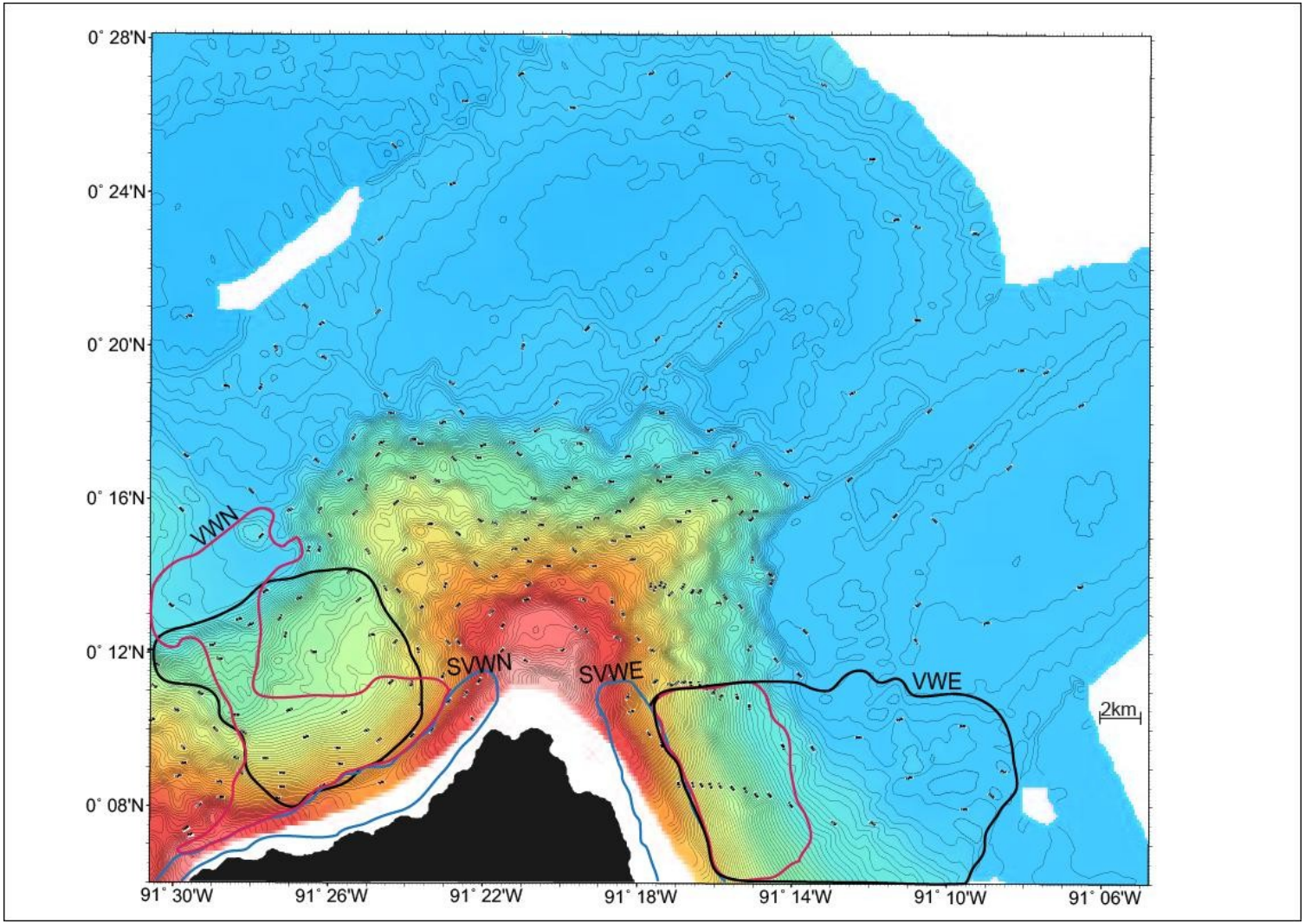

Figure 25. Volcan Wolf bathymetry contours with interpretations. Contour interval is 25 meters. Interpretations are the same as in Figure 24.

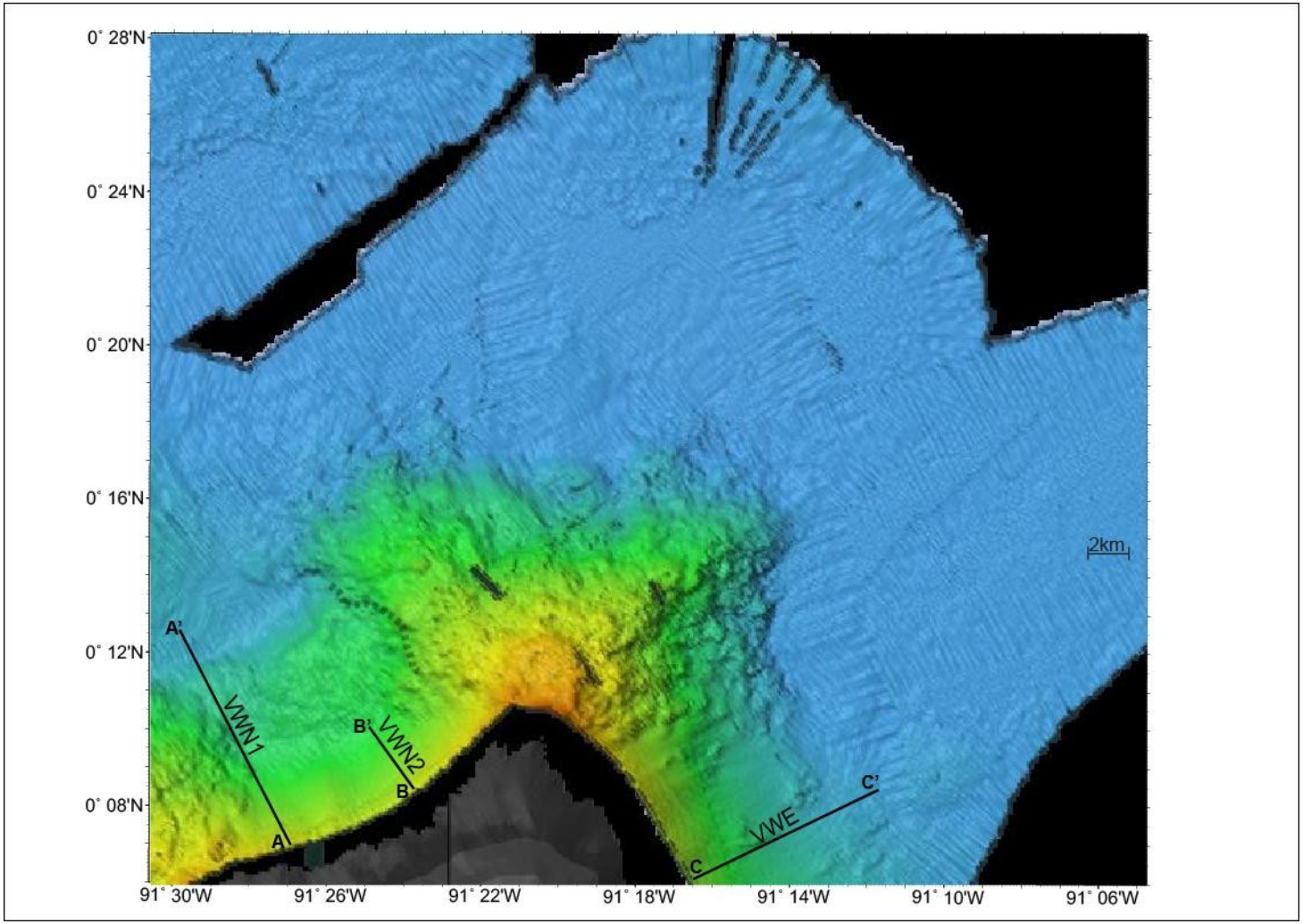

Figure 26. Volcan Wolf shaded relief bathymetry map. Illuminates the smooth bathymetry of the upper slopes and a hummocky texture on the lower slopes. This map also indicates the locations of scarps and cross section profiles A to A' and B to B' in the north and C to C' in the east.

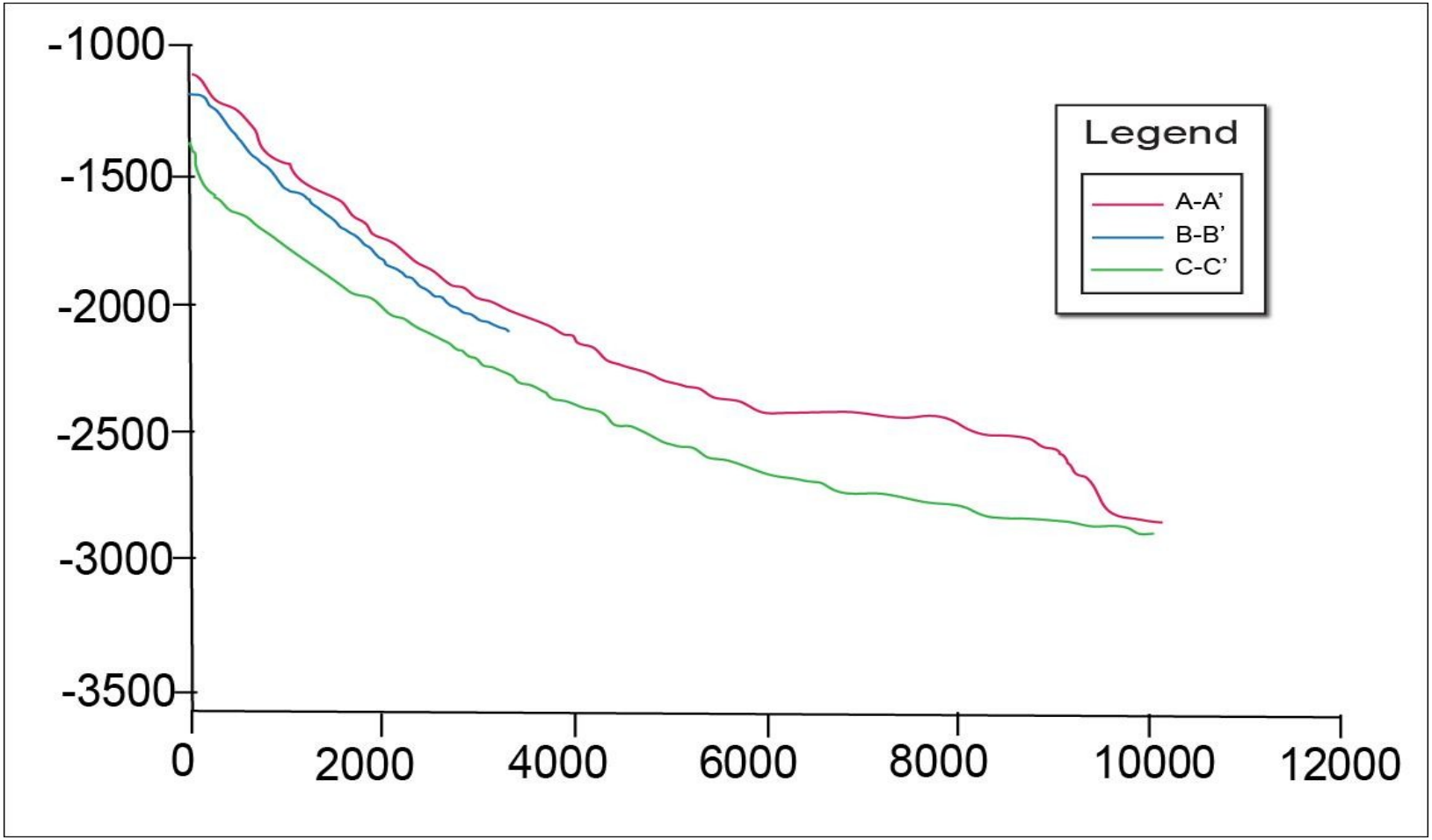

Figure 27. Volcan Wolf depth profiles. Shows the profile of A to A' in red with a hummocky texture that begins at ~2150 meters and continues to the base of the slide and a bulge that begins at ~2400 meters and continues to the base of the slide. Profile B to B' in blue shows the smooth texture of the upper slopes. Profile C to C' shows a hummocky texture which begins at ~200o meters and continues to the base of the slide. with a rough surface texture that begins at ~3000 meters of depth and continues to a depth of ~3600 meter, where there is a bulge.

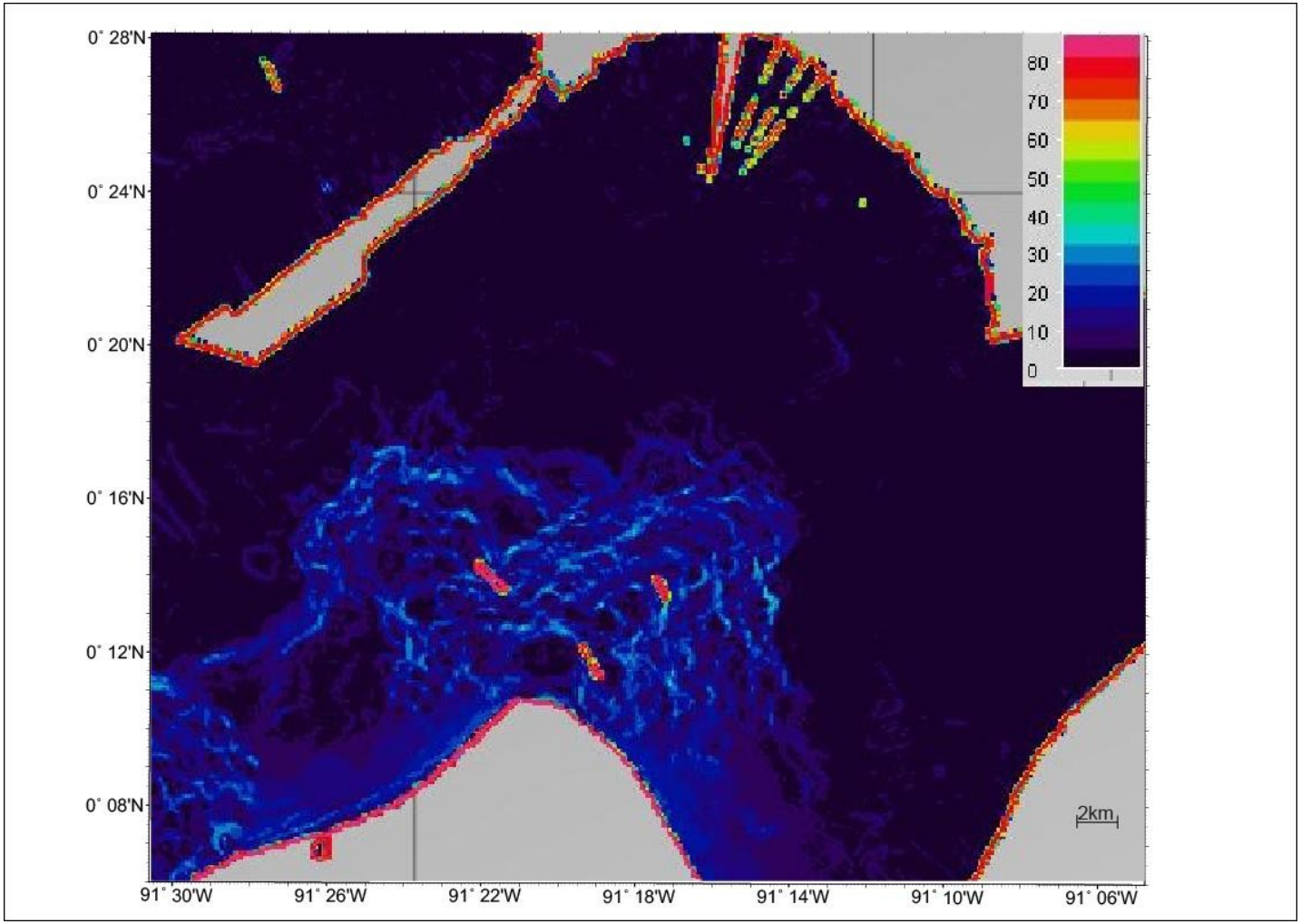

Figure 28. Volcan Wolf slope angle map. The slope angle map shows that the edges of the slide and the rift zone have a higher slope of ~30 degrees compared to the upper slopes of the slide area that have a 20 degree slope and shallow out with depth to nearly zero at the base of the slide.

the slide. The slope angle map shows this same bulge which is identifiable by an increase in slope (Figure 28). The slope angle map also shows that the edges of the slide and the surrounding rift zones have a higher slope of ~30 degrees compared to the upper slopes of the slide area that have a 20 degree slope and shallow out with depth to nearly zero at the base of the slide. This slide occurs off the concave north coast of Isabela, suggesting that the source for these deposits is subaerial.

VWE is located off the east coast of Isabela Island and ends in water depth of ~2975 meters. Based on sidescan sonar data, this slide extends for 5.7 km from the base of the slump sheets, has a maximum width of 9.7 km and an area of 57.2 km^2. Based on the bathymetry this slide extends for 16.3 km, has a maximum width of 10.3 km and an area of 162.9 km^2 as a minimum because the slides extends out of the data region. The shaded relief bathymetry map (Figure 26) indicates that the upper slopes have a smooth bathymetry while the lower slope has a hummocky morphology, which can be seen in depth profile C to C' (Figure 27). This profile also shows a general concave upward trend in the slope with a decrease in slope angle with increased water depth. The hummocky texture begins at ~2000 meters depth and continues to the interpreted base of the slide. The slope angle map shows that the edges of the slide and the rift zone have a higher slope of ~30 degrees compared to the upper slopes of the slide area that have a 20 degree slope and shallow out with depth to nearly zero at the base of the slide (Figure 28). This slide occurs in an isolated submarine embayment and has no apparent subaerial source.

3.6 Canal Isabela Region

The Canal Isabela region contains one large chaotic slump, SCI, which is identified by moderate backscatter amplitude with a mottled or speckled appearance in the sidescan sonar data (Figure 29). It has a length of 11.4 km, width of 13.6 km, and area of 70.1 km^2. The slump sheet is located to the east of Isabela Island and to the west of Santiago Islands within Canal Isabela which is located on the platform. The slump is identified by areas of hummocky terrain on the platform floor between the islands and by areas of concave contours on the upper slopes of Santiago Island in the bathymetry data (Figure 30). It has a length of 15.2 km, width of 13.8 km and area of 93.6 km^2. The shaded relief bathymetry map (Figure 31) shows the hummocky deposits between the islands and three scarps that appear on the upper slopes of Isabela Island and three scarps that are located on the upper slopes of Santiago Island as well as one scarp that is located across the side of one of the pointed cones identified by *Glass et al.* [2007]. The scarps that are on the upper slopes of Isabela Island are ~40 meters high. The scarps located on the upper slopes of Santiago Island range from 100 to 150 meters high. The scarp located on the pointed cone is ~20 meters high. Depth profile A to A' and B to B' both show a hummocky texture indicative of diffuse mass wasting across the canal (Figure 32). Profile B to B' shows a 125 meter high scarp that lies on the upper slopes of Santiago Island starting at 300 meters of depth. This profile also highlights the extremely steep slope of the island. The slope angle map shows that the upper slopes of Santiago and Isabela Islands are near 80 degrees while the platform between the islands has a slope near zero (Figure 33). This map also identifies ridges of higher slope within

the hummocky region which could be indicative of aggregation of materials from either a single large slide or multiple small slides. There is no clear source for this slump deposit.

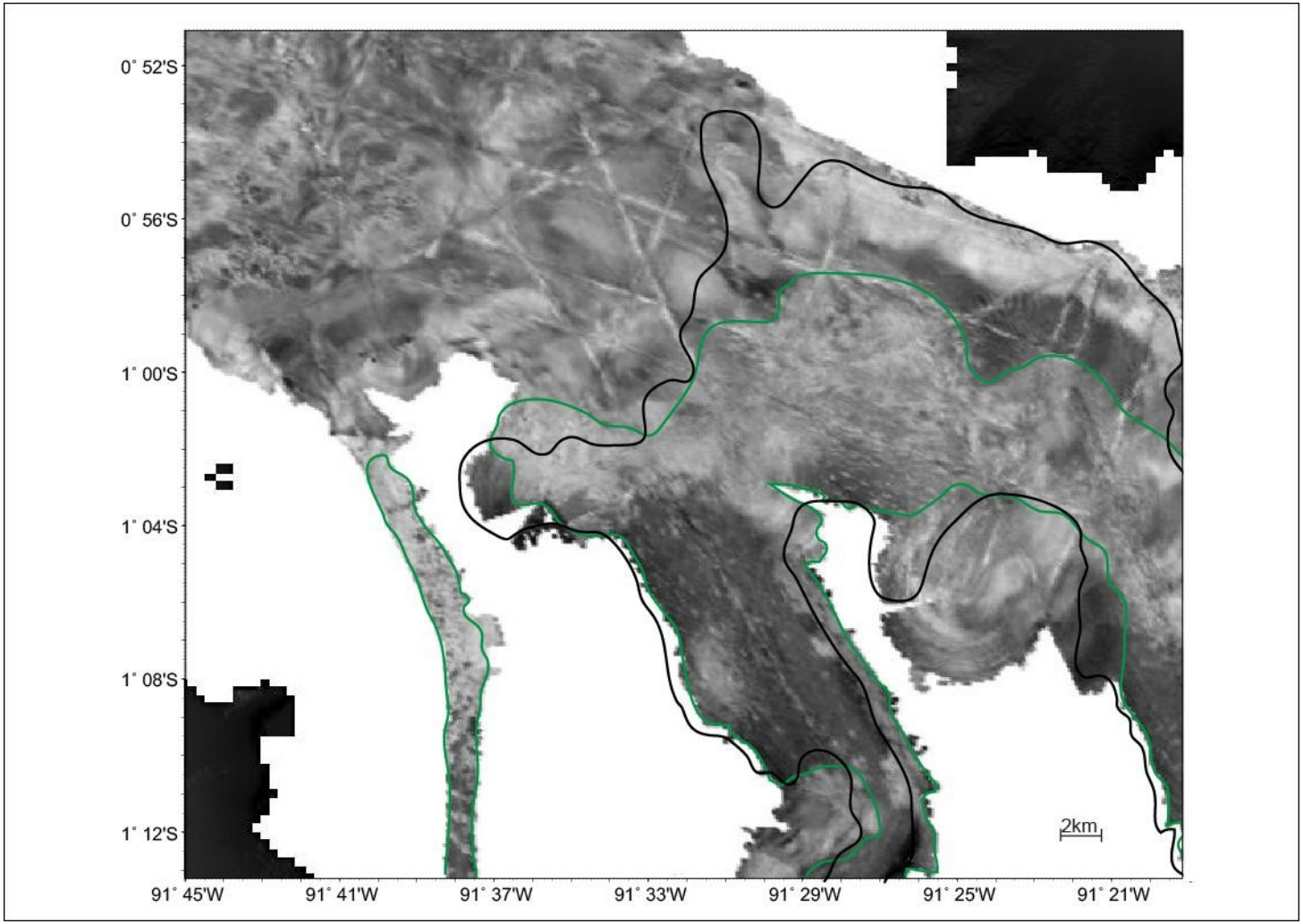

Figure 29. Canal Isabela sidescan sonar data interpreted. The area located to the east of Isabela Island and southwest of Santiago Island. Interpretations include chaotic slump outlined in green, with bathymetry interpretations outlined in black. Plot conventions as in Figure 4. Locations shown in Figure 3.

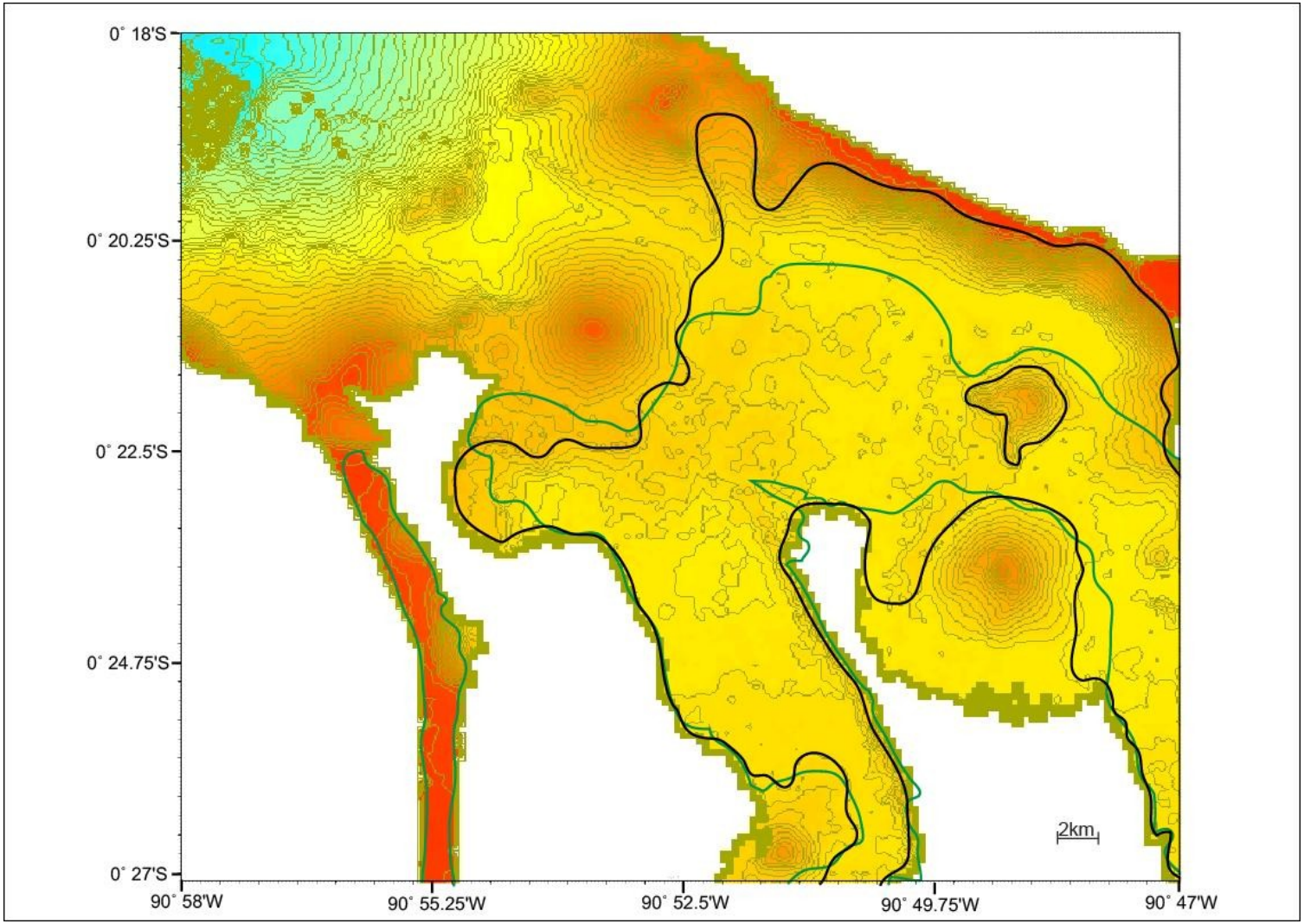

Figure 30. Canal Isabela bathymetry contours with interpretations. Contour interval is 25 meters. Interpretations are the same as in Figure 24.

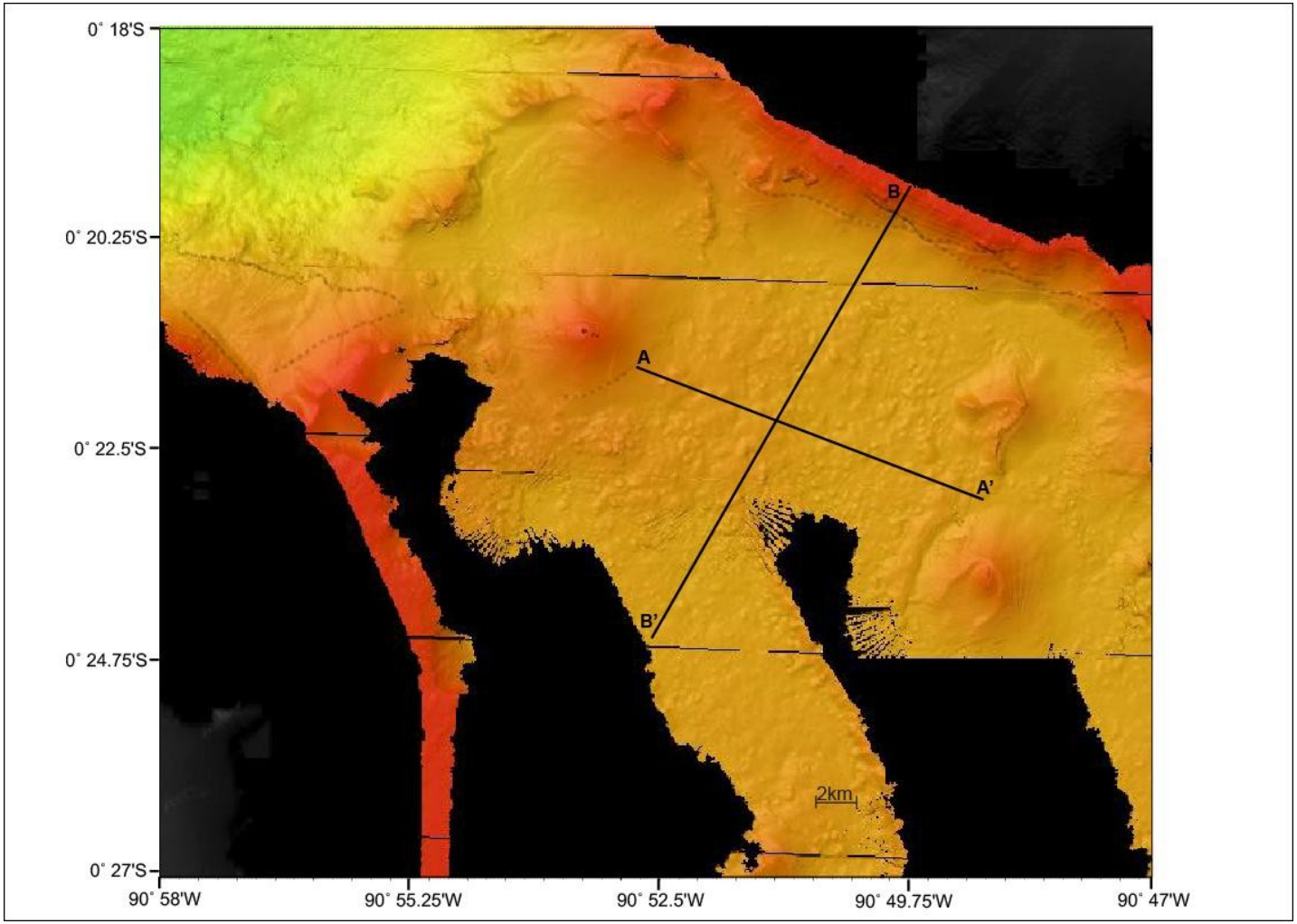

Figure 31. Canal Isabela shaded relief bathymetry map. Illuminates the hummocky texture of the canal floor and smooth upper slopes of the flanks of the islands. This map also indicates the locations of scarps and cross section profiles A to A' and B to B'.

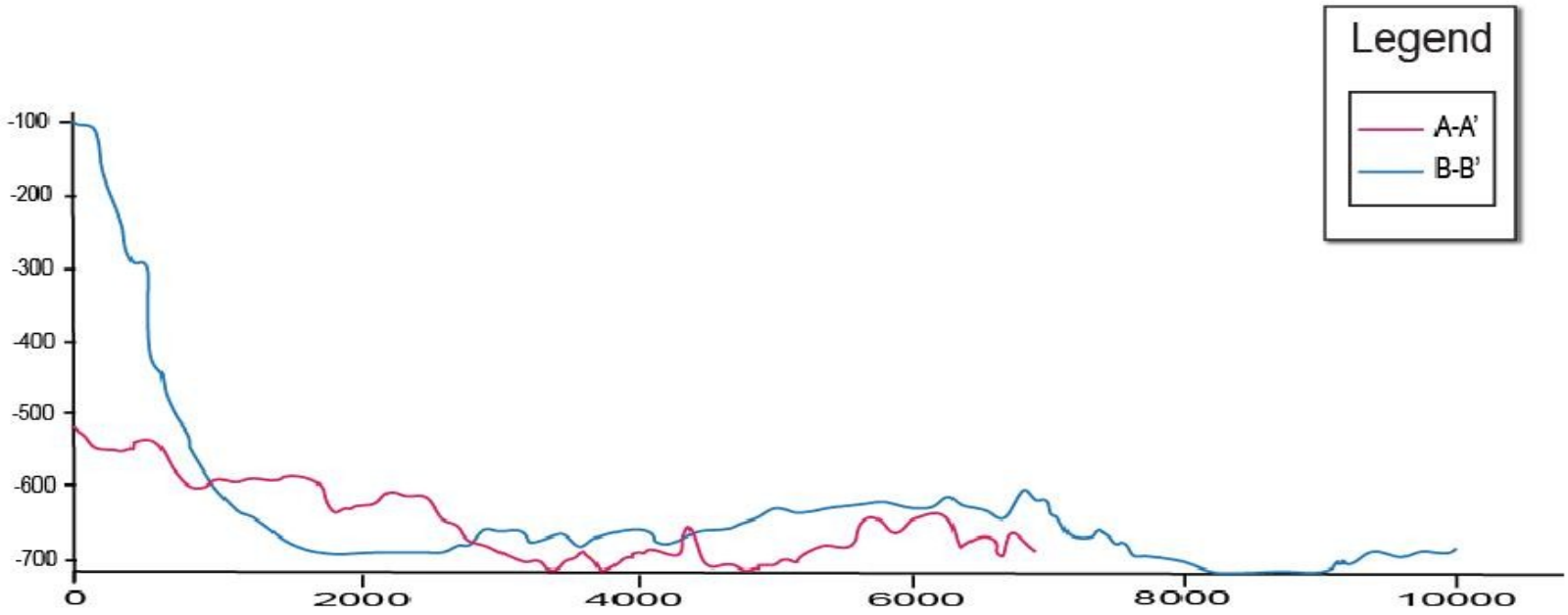

Figure 32. Canal Isabela depth profiles. Shows the profile of A to A' in red with a hummocky texture that continues along the full length of the canal. Profile B to B' in blue shows the smooth steep texture of the upper slopes as well as a 125 meter high scarp that lies on the upper slopes starting at 300 meters of depth. This profile also highlights the extremely steep slope of the island.

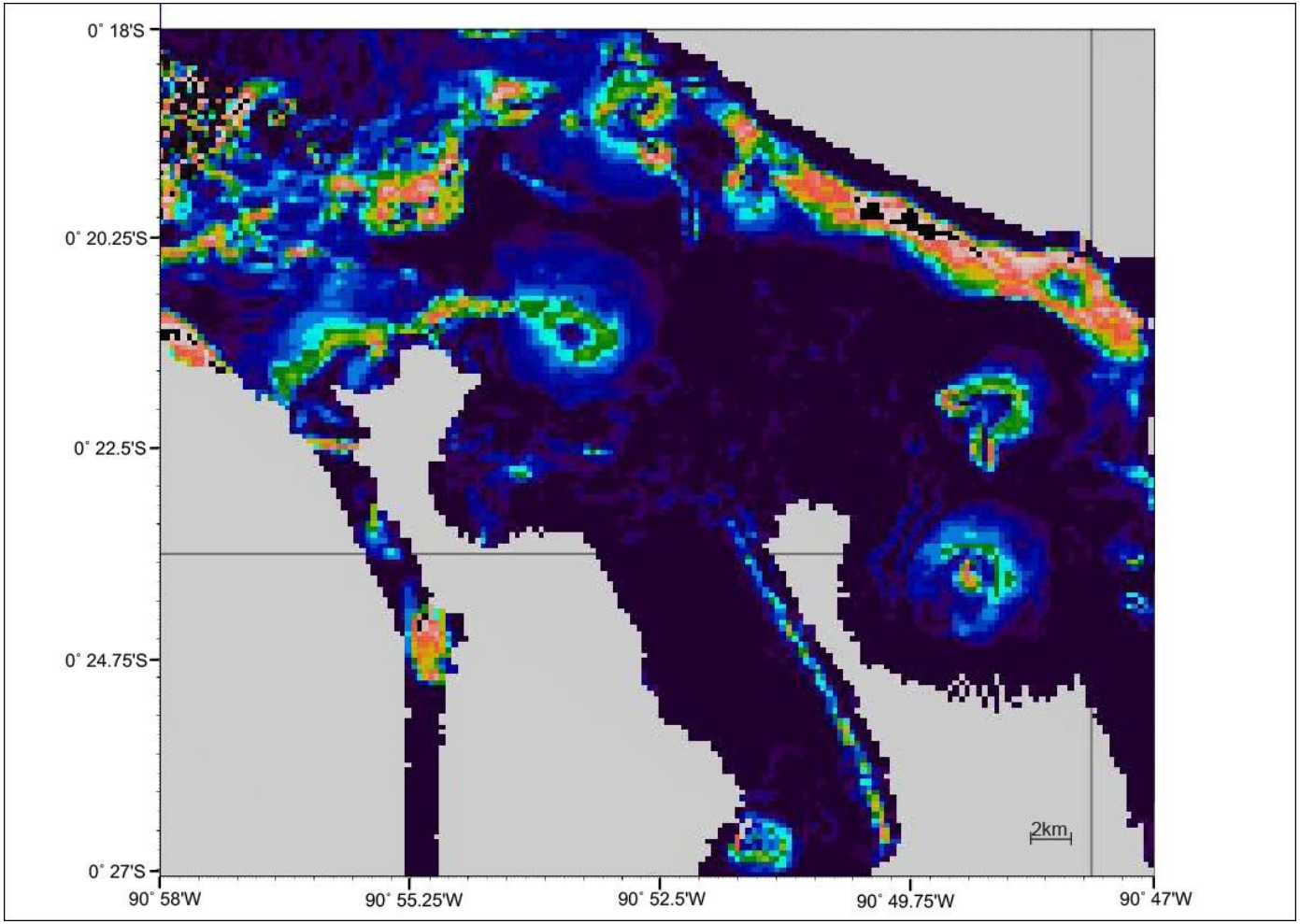

Figure 33. Canal Isabela slope angle map. The slope angle map shows that the upper slopes of Santiago Island and Isabela Island are near 80 degrees while the platform between the islands has a slope near zero. This map also identifies ridges of higher slope within the hummocky region which could be indicative of aggregation of materials from either a single large slide or multiple small slides.

4. DISCUSSION

Approximately 73 percent of the coastlines of the western Galapagos Islands have been affected by some form of downslope movement. Debris flows affect ~64 of lower slopes of the western Galapagos. This indicates that, at least at the western edge of the platform, mass wasting plays a significant role in the development of these volcanoes. The flanks of the southwestern and northern tips of Isabela Island and the west flank of Fernandina Island lie at the unbutressed edge of the Galapagos platform. The growth of the islands on this steep edge may lead to an increased instability of the submarine flanks, causing unstable deposits on over-steepened slopes. This observation would lead one to believe that the western Galapagos may be more susceptible to mass wasting along this edge when compared to the rest of the archipelago platform.

Geist et al. [2006] identified only four areas of mass wasting to the west and north of Fernandina Island, but this study has found that a total of 23 mass wasting features were found to exist in the western Galapagos Islands. Of the nine types of mass wasting identified by *Coleman and Prior* [1988], *Moore et al*.[1989], and *Keating et al.*[2000], only four types are observed in the sonar imagery of the western Galapagos Islands. Fourteen debris flows with one that incorporated a set of detached blocks, seven slump sheets, and one chaotic slump were interpreted.

The average slide in the western Galapagos Islands is identified by downslope lineations in the sidescan sonar images, has concave contours on the upper slopes and a fanning of the contours (convex contours) at the base of the slope in the bathymetry, is located within a horseshoe shaped embayment and has a generally concave upward trend

in the slope with a decrease in slope angle with increased water depth and a hummocky texture towards the distal end of the slide.

Twelve of the fourteen interpreted debris flows are flanked by submarine rift zones ridges identified by *Geist et al.* [2006] and *Glass et al.* [2007]. The existence of these rift zones ridges has generated a concave area of the submarine slope between the rifts. The combination of the concave regions between rifts mixed with dike intrusions, earthquakes, and magma chamber inflation and deflation within the rifts may lead to a weakening of these concave areas, causing it to be more susceptible to downslope movement. The slides that exist within these concave or horseshoe shaped embayments are most likely to be a product of mass wasting due to these geological processes. In the sedimentary record, repeated landslides would be bounded above and below by large accumulations of sediments that would be horizontal, while the slide deposits would be a discontinuous chaotic mass of volcanic origin. The slides that do not exist within these horseshoe shaped embayments are most likely produced due to continuous erosional processes on the steep upper slopes of the islands. The small repeated failures of the flanks would likely lead to small, thin and continuous mass wasting events instead of large thick individual slides. These continuous events will lead to a thicker accumulation of deposits.

The western Galapagos Islands are still in the beginning shield building stages and continued volcanism at the western edge of the Galapagos platform, both submarine and subaerial, act to resurface and conceal the submarine terrain and therefore other evidence of mass wasting, such as the existence of thick slides deposits and headwall

scarps. Slides that have more sharply defined edges are younger and have been affected less by continued volcanism.

Sidescan sonar and bathymetry definitions of the slides' lengths, widths and areas are different. The bathymetry definitions are generally larger than the sidescan sonar definitions indicating that the sidescan sonar measurements have been decreased due to covering by continued volcanism. An example of this can be seen in both Figure 4 and Figure 24 where a large deep water lava flow, an irregularly shaped area of higher reflectivity, exists within the region of the slide which is defined by the bathymetry. This causes the area of the slide defined by sidescan sonar to be smaller than the area defied by bathymetry. This indicates that sidescan sonar detection of mass wasting features will only be able to determine minimum measurements.

When compared to the Hawaiian Islands, the areas and lengths of slides interpreted along the western Galapagos are significantly less. *Moore et al*.[1989] describes more than 68 major slides along the full axis of the Hawaiian Ridge, each more than 20 km long, and cover about one half of the flanks of the ridge. *Watts and Mason* [1995] identified a giant landslide on the north flank of Tenerife, Canary Islands that was ~ 100 km long and 80 km wide. These giant slides, imaged by GLORIA, have been determined to occur through all stages of volcano shield building. Though the numerous and large volume slides of the Hawaiian and Canary Islands are not mirrored in the bathymetry of the western Galapagos, the existence of subaerial sector collapse scars, like that of Volcan Ecuador, the proximity of the platform to the abyssal plain, and the growth of the islands on the steep platform edge suggest that larger mass wasting

events may have occurred in the history of the Galapagos Islands, but that the evidence for such events lie outside of the study area or has been masked by the submarine volcanism. *Geist et al*. [2002] explains that catastrophic sector collapse(s) of Volcan Ecuador's western flank most likely slid to abyssal depths off the platform evidenced by the existence of hummocky terrain, primarily obscured by young lava flows, to a distance of 20 km from the west coast. Other sector collapses known to occur in the western Galapagos, including the southwest flank of Cerro Azul [*Naumann and Geist*, 2000], the west face of Pinta [*Cullen and McBirney*, 1987] and the west face of Santa Fe [*Geist et al*., 1985] indicate that giant slides are likely.

The maximum resolution of the bathymetry data is 25m. The thickness of mass wasting features could not be determined in the bathymetry because the thicknesses were unable to be differentiated reliably from the original shape of the volcano. Additional data, such as sub-bottom or seismic profiles will be necessary to determine the thickness of the slides and their respective volumes. The uncertainty in the slide definition is variable because another person may decide to draw the edges of the slide differently because their perception of the slide bounds may be different.

5. CONCLUSION

Four types of mass wasting have been identified in the western Galapagos Island including slump sheets, debris flows, detached blocks, and chaotic slumping. A total of 23 mass wasting features were found to exist in the western Galapagos Islands, including fourteen debris flows with one that incorporated one set of detached blocks, seven slump sheets, and one chaotic slump with hummocky terrain. Some of the indentified features have obvious origination zones while the sources of others are not clearly identifiable. Approximately 73 percent of the surveyed coastlines are affected by slumping on the steep upper slopes and ~64 percent are affected by debris flows on the lower slopes. Unlike the giant landslides documented by GLORIA imagery around the Hawaiian Islands, the western Galapagos Islands appear to be characterized by small slump sheets existing along the steep shallow submarine flanks of the island and by debris flows that are flanked by rift zones and extend off the platform. The slumps have areas ranging from 13.6 km^2 to 93.7 km^2, lengths varying from 4.4 to 36.3 km and widths ranging from 1.2 to 2.5 km. These debris flows range from 4.0 to 15.4 km at their widest point and are less than 17 km long. This study indicates that submarine mass wasting is widespread in the western Galapagos, suggesting that the production of small-scale downslope movement is part of the erosive nature of these oceanic volcanic islands.

REFERENCES

Bailey, K., (1976), Potassium-Argon ages from the Galapagos Islands, *Science*, *192*(4238), 465-467, DOI:10.1126/science.192.4238.465.

Borgia, A., (1994), Dynamic basis of volcanic spreading, *Journal of Geophysical Research*, *99*(B9), 17791-17804, DOI: 10.1029/94JB00578.

Coleman, J., and D. Prior (1988), Mass wasting on continental margins, *Annual Review of Earth and Planetary Sciences*, *16*, 101-119, DOI: 10.1146/annurev.ea.16.050188.000533.

Cullen, A., and A. McBirney (1987), The volcanic geology of petrology of Isla Pinta, Galapagos Archipelago, *Geological Society of America Bulletin, 98*, 294-301, DOI: 10.1130/0016-7606(1987)98.

Elsworth, D., and B. Voight (1995), Dike intrusion as a trigger for large earthquakes and failure of volcano flanks, *Journal of Geophysical Research*, *100*, 6005-6024.

Firth, C., I. Stewart, W. McGuire, S, Kershaw, and C. Vita-Finzi (1996), Coastal elevation changes in eastern Sicily: Implications for volcano instability at Mount Etna, in McGuire W., P. Jones, and J. Neuberg (eds) Volcano instability on the Earth and other planets, *Geological Society [London] Special Publication*, *110*, 153-167, DOI: 10.1144/GSL.SP.1996.110.01.1.

Fornari, D., J. Moore, and L. Calk (1979), A large submarine sand rubble flow on the Kilauea Volcano, Hawaii, *Journal of Volcanology and Geothermal Research*, *5*(3-4), 239-256, DOI: 10.1016/0377-0273(79)90018-0.

Fornari, D., M. Kurz, D. Geist, P. Johnson, G. Peckman, and D. Scheirer (2001), New perspectives on the structure and morphology of the submarine flanks of Galapagos volcanoes – Fernandina and Isabela, *EOS Trans. AGU*, *82*(47), Fall Meet. Suppl., Abstract T41D-06.

Geist, D., A. McBirney, and R. Duncan (1985), Geology of Sante Fe Island: The oldest Galapagos Volcano, *Journal of Volcanology and Geothermal Research, 52*, 65-82, DOI: 10.1016/0377-0273(85)90056-3.

Geist, D., W. White, F. Albarede, K. Harpp, R. Reynolds, J. Blichert-Toft, and M. Kurz. (2002), Volcanic evolution in the Galapagos: The dissected shield of Volcan Ecuador. *Geochemistry Geophysics Geosystems*, *3*(10), 1061, DOI: 10.1029/2002GC000355.

Geist, D., T. Naumann, J. Standish, M. Kurz, K. Harpp, W. White, and D. Fornari (2005), Wolf Volcano, Galapagos Archipelago: Melting and magmatic evolution at the margins of a mantle plume, *Journal of Petrology*, *46*(11), 2197-2224, DOI: 10.1093/petrology/egi052.

Geist, D., D. Fornari, M. Kurz, K. Harpp, S. Adam Soule, M. Perfit, and A. Koleszar (2006), Submarine Fernandina: Magmatism at the leading edge of the Galapagos hot spot, *Geochemistry Geophysics Geosystems, 7*(12), CiteID Q12007, DOI: 10.1029/2006GC001290.

Gillot, P., J. Lefevre, and P. Nativel (1994), Model for the structural evolution of the volcanoes of Reunion Island, *Earth Planetary Science Letter*, *122*, 291-302, DOI: 10.1016/0012-821X(94)90003-5.

Glass, J., D. Fornari, H. Hall, A. Cougan, H. Berkenbosch, M. Holmes, S.White, and G. De La Torre (2007), Submarine geomorphology of the western Galapagos based on EM-300 bathymetry and MR1 side-scan sonar, *Geochemistry Geophysics Geosystems*, *8*(3), CiteID Q03010, DOI: 10.1029/2006GC001464.

Gripp, A., and R. Gordon (2002), Young tracks of hot-spots and current plate velocities, *Geophysical Journal International*, *150*, 321-361.

Hampton, M., H. Lee, and J. Locat (1996), Submarine Slides, *Reviews of Geophysics*, *34*, 33-59.

Harpp, K., D. Fornari, D. Geist and M. Kurz (2003), Genovesa Submarine Ridge: A manifestation of plume-ridge interaction in the northern Galapagos Islands, *Geochemistry Geophysics Geosystems*, *4*(9), 8511, DOI: 10.1029/2003GC000531.

Holcomb, R., and R. Searle (1991), Large slides from oceanic volcanoes, *Marine Geotechnology*, *10*(1-2), 19-32, DOI: 10.1080/10641199109379880.

Keating, B., C. Helsley, and I. Karogodina (2000), Sonar studies of submarine mass wasting and volcanic structures off Savaii Island, Samoa, *Pure and Applied Geophysics*, *157*(6-8), 1285-1313, DOI: 10.1007/s000240050026.

Kurz, M., D. Fornari, D. Geist, and Shipboard Scientific Party (2001), *Cruise report Leg-4 R/V Roger Revelle*, National Science Foundation Ocean Sciences Division Marine Geology & Geophysics OCE – 0002461.

Lenat, J., P. Vincent, and P. Bachelery (1989), The off-shore continuation of an active basaltic volcano: Piton de la Fournaise (Reunion Island, Indian Ocean); Structural and geomorphological interpretation from seabeam mapping, *Journal of Volcanology and Geothermal Research.*, *36*(1-3), 1-36, DOI: 10.1016/0377-0273(89)90003-6.

Lo Giudice, E., and R. Rasa (1992), Very shallow earthquakes and brittle deformation in active volcanic areas: The Etnean region as an example, *Tectnophysics*, *202*(2-4), 257-268, DOI: 10.1016/0040-1951(92)90111-I.

McGuire, W., A. Pullen, and S. Saunders (1990), Recent dyke-induced large scale block movement at Mount Etna and potential slope failure, *Nature*, *343*, 357 – 359, DOI: 10.1038/343357a0.

McGuire, W. (1996), Volcano instability: A review of contemporaneous themes, in McGuire W., P. Jones, and J. Neuberg (eds), Volcano Instability on the Earth and other planets, *Geological Society [London] Special Publication*, *110*, 1–23.

Montalto, A., S. Vicinguerra, S. Menza, and G. Patane (1996), Recent seismicity of Mount Etna: Implication for flank instability, *Geological Society [London] Special Publications*, *110*, 169-177, DOI: 10.1144/GSL.SP.1996.110.01.13

Moore, J. (1964), Giant Submarine slides on Hawaiian Ridge, *U.S. Geological Survey Open File Rep.*, *501-D*, D95-D98.

Moore, J., D. Clague, R. Holcomb, P. Lipman, W. Normark, and M. Torresan (1989), Prodigious submarine slides on Hawaiian Ridge, *Journal of Geophysical Research*, *94*, 17484-17645.

Murray, J., and B. Voight (1996), Slope stability and eruption prediction on the eastern flank of Mount Etna, *Geological Society [London] Special Publication*, *110*, 111-114, DOI: 10.1144/GSL.SP.1996.110.01.08.

Naumann, T., and D. Geist (2000), Physical volcanology and structural development of Cerro Azul volcano, Isabela Island, Galapagos: Implications for the development of Galapagos-style shield volcanoes, *Bulletin Volcanology*, *61*(8), 497-514, DOI: 10.1007/s004450050008.

Simkin, T. (1984), Geology of the Galapagos Islands, in *Galapagos (Key Environments)*, edited by R. Perry, 15–41, Elsevier, New York.

Simkin, T., and L. Siebert (1994), *Volcanoes of the World, 2nd ed.*, 349, Geoscience Press, Arizona.

Stillman, C. (1999), Giant Miocene slides and the evolution of Fuerteventura, Canary Islands, *Journal of Volcanology and Geothermal Research*, *94*, 89-104, DOI: 10.1016/S0377-0273(99)00099-2.

Watts, A., and D. Masson (1995), A giant slide on the north flank of Tenerife, Canary Islands, *Journal of Geophysical Research*, *100*, 24487-24498.

Wilson, D., and R. Hey (1995), History of rift propagation and magnetization intensity for the Cocos-Nazca spreading center, *Journal of Geophysical Research*, *100*(B7), 10041-10056, DOI: 10.1029/95JB00762.

VITA

Name: Hillary Fawn Hall

Address: In care of the Department of Oceanography
Texas A&M University
Eller O&M Building
MS 3146
College Station, TX 77843-3146

Email Address: hallh11@gmail.com

Education: B.S., Oceanography, The University of Washington at Seattle, 2006

B.S., Earth and Space Sciences, The University of Washington at Seattle, 2006

M.S., Oceanography, Texas A&M University, 2011

Publications and presentations:

Glass, J., D. Fornari, **H. Hall**, A. Cougan, H. Berkenbosch, M. Holmes, S.White and G. De La Torre (2007), Submarine geomorphology of the western Galapagos based on EM-300 bathymetry and MR1 side-scan sonar, *Geochemistry Geophysics Geosystems*, *8*(3), CiteID Q03010, DOI: 10.1029/2006GC001464.

Hall, H., W. Sager (2009), Mass Wasting of the Western Galapagos. American Geophysical Union Fall Meeting, Abstract #NH41C-1261 and poster presentation**.**